David Taylor Research Center
Bethesda, MD 20084–5000

DTRC–PAS–91/55 February 1992

Propulsion and Auxiliary Systems Department
Research and Development Report

The Application of Unsteady Potential Flow Vortex Loop/Dipole Theory to the Work and Acoustics of Low-Speed Turbomachinery

by
Earl Quandt

DTRC–PAS–91/55 The Application of Unsteady Potential Flow Vortex Loop/Dipole Theory to the Work and Acoustics of Low-Speed Turbomachinery

MAJOR DTRC TECHNICAL COMPONENTS

CODE 011 DIRECTOR OF TECHNOLOGY, PLANS AND ASSESSMENT

12 SHIP SYSTEMS INTEGRATION DEPARTMENT

14 SHIP ELECTROMAGNETIC SIGNATURES DEPARTMENT

15 SHIP HYDROMECHANICS DEPARTMENT

16 AVIATION DEPARTMENT

17 SHIP STRUCTURES AND PROTECTION DEPARTMENT

18 COMPUTATION, MATHEMATICS & LOGISTICS DEPARTMENT

19 SHIP ACOUSTICS DEPARTMENT

27 PROPULSION AND AUXILIARY SYSTEMS DEPARTMENT

28 SHIP MATERIALS ENGINEERING DEPARTMENT

DTRC ISSUES THREE TYPES OF REPORTS:

1. **DTRC reports, a formal series,** contain information of permanent technical value They carry a consecutive numerical identification regardless of their classification or the originating department.

2. **Departmental reports, a semiformal series,** contain information of a preliminary, temporary, or proprietary nature or of limited interest or significance. They carry a departmental alphanumerical identification.

3. **Technical memoranda, an informal series,** contain technical documentation of limited use and interest. They are primarily working papers intended for internal use. They carry an identifying number which indicates their type and the numerical code of the originating department. Any distribution outside DTRC must be approved by the head of the originating department on a case-by-case basis.

David Taylor Research Center
Bethesda, MD 20084–5000

DTRC–PAS–91/55 February 1992
Propulsion and Auxiliary Systems Department
Research and Development Report

The Application of Unsteady Potential Flow Vortex Loop/Dipole Theory to the Work and Acoustics of Low Speed Turbomachinery

by
Earl Quandt

CONTENTS

FIGURES

LIST OF SYMBOLS
ENGLISH LETTERS

Symbol	Meaning	Units
A	Surface area	L^2
a	Spacing	L
B	Number of blades, Fourier Coeff.	–
c	Speed of sound	L/T
D	Dipole strength	L^2/T
F	Force	F
f	Force per volume	F/L^3
G	Green's dipole strength	L^4/T
H	Total enthalpy	L^2/T^2
h	Blade span	L
I	Impulse	FT
i	Unit vector	–
J	Bessel function	–
j	Unit vector or integer index	–
k	Wave number, or integer index	1/L
l	Distance variable	L
M	Mach number	–
m	Integer index	–
m	Mass addition rate per volume	$M/L^3\,T$
n	Unit vector or integer index	–
P	Power	FL/T
p	Pressure	F/L^2
Q	Volume addition rate	L^3/T
q	Vane index number	–
R	Radius of sphere	L
r	Radial position coordinate	L
S	Surface area	L^2
s	Position coordinate to surface	L
T	Period for repetition	T
t	Time	T
U	Velocity	L/T

u	Velocity component	L/T
V	Velocity in absolute frame	L/T
v	Velocity component	L/T
V	Volume	L^3
W	Velocity in rotating frame	L/T
x	Position coordinate	L
y	Position coordinate	L
z	Position coordinate	L

GREEK LETTERS

Symbol	Meaning	Units
β	Angle from z axis	–
Γ	Vortex strength	L^2/T
Δ	Volume or a difference	L^3
δ	Small difference	–
ϕ	Velocity potential	L^2/T
μ	Fluid viscosity	FT/L
ρ	Fluid density	M/L^3
θ	Circumferential angle	–
τ	Time	T
ζ	Fluid vorticity = $\vec{\nabla} \times \vec{V}$	1/T
Ω	Shaft radian rotation rate	1/T
ω	Radian frequency	1/T
∇	Operational derivative symbol	1/L

SUBSCRIPTS

Symbol	Meaning
a	Acoustic
A	Added mass
N	Normal
o	Observer
Rel	Relative
D	Dipole
v	Vortex

ABSTRACT

An ideal turbomachine transfers energy from a rotating shaft to a fluid through the creation of a flow field that is unsteady in the absolute frame. In order to understand and control the work and acoustics of this process the basic building-block singularities of potential flow are developed in a unified manner such that both near- and far-field effects appear naturally in the formulation. It is shown how the total vector force applied to the fluid by a discrete rigid blade is related to the bound and shed vortex system and the acceleration of the displaced mass. Following Lighthill, the volume integral of the vector moment of vorticity is found to describe most fundamentally how the unsteady fluid motions in a turbomachine are related to surface forces that do work on the fluid.

Because unsteady flow is required for energy transfer, the work input of a single blade creates simultaneously in the fluid an acoustic signal that propagates to the far-field. The strength of this signal is determined by the time derivative of the instantaneous blade force component in the direction of a stationary observer, i.e., with the pattern of a rotating dipole. The summation of these tonal signals from combinations of blades and vanes is computed for free-field and cylindrical duct boundary conditions. Bessel functions are found to characterize both cases, their order being determined by specific blade/vane number differences. Rules for tonal sound control by acoustic interference or mode decay, such as those of Tyler and Sofrin, are examined. Implications for broadband acoustics are discussed.

The ideal unsteady singularity concepts are extended to turbomachines having centrifugal and real fluid effects. It is concluded that this unified vortex/dipole approach provides a sound basis for continued turbomachinery understanding and developments.

ADMINISTRATIVE INFORMATION

This report was prepared by the research staff of the Propulsion and Auxiliary Systems Department (Code 27) of the David Taylor Research Center (DTRC) for the purpose of organizing the theoretical knowledge relating to a machinery component common to several department projects. It was supported by department overhead funds.

INTRODUCTION

The mathematics of potential flow represent a simple, yet effective, analysis tool that can provide an accurate initial understanding of many three-dimensional time-varying flows. Moreover, this technique has the desirable property that solutions are additive so that particular phenomena can be studied separately in simple form, and then summed to represent complex cases. One such case is the turbomachine, which is made up of a set of discrete air-foil shaped blades rotating in a three-dimensional flow field. From the thermodynamic stand point this machine receives input through a shaft that rotates at (generally) constant speed and experiences a (generally) constant torque and thrust. As a result, the machine adds, or subtracts, work from the moving fluid, and may also give propulsive thrust to a vehicle. Using the building block property of potential flow theory, two-dimensional, three-dimensional, and unsteady flows can be examined separately and in combination. For turbomachines it is especially revealing to simulate the motion of the blades, and the resulting time-varying velocity fields, as seen by a fixed observer in order to account mathematically for the work done on the fluid. But, beyond the work, and as a

usually unwanted side effect, the blade motion also initiates acoustic signals in the fluid, which propagate at the speed of sound over great distances. Since most acoustic analyses are based on potential flow theory, it is the goal of this study to develop a potential flow description of the fundamental machine work process that leads directly to a unified technique for characterizing the sound field associated with the work.

The concepts developed herein are an extension of an earlier study by this author. That study demonstrated the advantage of using unsteady potential flow vortex fields to describe the work and acoustic signature of an axial flow rotor in a three-dimensional free field. Since that initial investigation, it has been found useful to explore further the theory, to consider centrifugal effects, and to include the details of acoustic interference of rotor-stator combinations in open and ducted environments. In applying the theory, this study builds on the fluid dynamic principles presented by Lamb, since that is the classic treatment of potential flow and basic acoustics. Another very helpful, and contemporary, source of background is the work of Lighthill, both for potential flow and acoustics. Other singular contributions are also used, such as Preston for the moving vortex-work analysis, Gutin for the original acoustic interference theory, Tyler and Sofrin for the rotor-stator acoustics, and Goldstein, Cumpsty and Blake for their comprehensive summaries of the Aero-Hydro Acoustics of turbomachines.

It is therefore the purpose of this report to present the essential aspects of unsteady potential flow vortex systems so as to provide a complete and consistent description of the work and acoustic behavior of low speed turbomachines. The condition of "low speed" is used both to eliminate the need to consider significant fluid compressibility, and to require that acoustic signals generated over any given time interval will have propagated distances much greater than a blade dimension or movement in that same time. In addition, all effects are considered to occur without fluid viscosity, without turbulence, and with rigid stationary and moving surfaces. The following pages describe how the work-related parts of turbomachine time-varying velocity fields are viewed best as expanding three-dimensional vortex loops, or equivalently, to injected dipoles; how the important features of displaced and added mass arise for an oscillating rigid sphere dipole; how multisource acoustic interference develops from multiple blades in a free-field and in a duct environment; and how the basic vortex/dipole concept can give insight into even more complex turbomachine behavior.

BLADE VORTEX LOOPS, DIPOLES AND WORK

THE UNSTEADY VELOCITY POTENTIAL AND ENTHALPY

In order to apply the mathematics of potential flow it is necessary to assume that the fluid have no viscosity and be in irrotational motion, i.e., $\mu = 0$ and the vorticity, $\zeta = 0$ throughout the flow field. These two restrictions are acceptable for many flows and are often related since viscosity generates rotation in an otherwise irrotational field. When these conditions are met, and the fluid is essentially incompressible, it is possible to express the velocity anywhere in the flow field in terms of the gradient of a scalar. Thus the equation for the conservation of mass in the fluid becomes Laplace's equation, solutions to which require only boundary conditions. Hence,

$$\phi = \phi(x,t) \text{ and } \vec{V} = \vec{\nabla}\phi, \text{ then } \vec{\nabla} \cdot \vec{V} = 0 = \nabla^2\phi \qquad (1)$$

Therefore ϕ is termed the "velocity potential" of a flow field, with the convenient property that multiple potentials can be summed to represent more and more complex flows. One of the building block potentials that describes circular motions is that of the vortex at the origin, which, for a two dimensional field is simply;

$$\phi_v = \frac{\Gamma}{2\pi}\theta \tag{2}$$

Here θ is an angle measured from some reference axis, and Γ is the strength of the vortex. Applying Eq. (1), the two-dimensional velocity components are:

$$v_r = \frac{\partial \phi_v}{\partial r} = 0 \quad \text{and} \quad v_\theta = \frac{1}{r}\frac{\partial \phi_v}{\partial \theta} = \frac{\Gamma}{2\pi r} \tag{3}$$

Thus the radial velocity is zero and the circular velocity varies inversely with the radius, being singular, i.e. infinite, at the origin. It can be seen that a line integration of the velocity around any closed loop that includes the singularity gives the value Γ. Because of this, the velocity potential of the vortex can be seen to have the rather unique property that it increases by this value for any 2π change in angle, *a behavior most important for simulating turbomachine force and work effects.*

In addition to the conservation of mass, the conservation of linear momentum must also be satisfied for any flow system, i.e.,

$$\frac{\partial \vec{V}}{\partial t} = -\frac{1}{\varrho_o}\vec{\nabla}p - \vec{\nabla}\left(\frac{V^2}{2}\right) - \vec{\xi} \times \vec{V} + \frac{\mu}{\varrho_o}\nabla^2\vec{V} \tag{4}$$

For potential flow of an incompressible fluid this equation can be simplified to the unsteady Bernoulli form.

$$\vec{\nabla}\left(\frac{\partial \phi}{\partial t}\right) = -\vec{\nabla}\left(\frac{p}{\varrho_o} + \frac{V^2}{2}\right) = -\vec{\nabla}(H_T) \tag{5}$$

Therefore a gradient in fluid total enthalpy, which is the purpose of a turbomachine, is associated directly with a gradient in the time variation of the velocity potential. If the vortex of Eq. (2) is steady in time, then the total enthalpy is uniform throughout the flow field, giving;

$$p + \varrho_o\left(\frac{V^2}{2}\right) = const. \tag{6}$$

A SINGLE MOVING 2–D VORTEX

Usually, the static pressure at $r = \infty$ is fixed, at say zero, then the pressure at the origin will be $-\infty$. If then the vortex is allowed to translate, say in the –x direction with velocity U_T, the behavior of total enthalpy with respect to the absolute frame is;

$$\frac{\partial \phi}{\partial t} = \frac{\Gamma}{2\pi} \tan^{-1}\left(\frac{y}{x + U_T t}\right) = -\frac{\Gamma}{2\pi} \frac{U_T}{r_{rel}} \sin\theta_{rel} = -U_T U_{rel} = -H_T \quad (7)$$

where θ_{rel} and r_{rel} are measured from the center of the moving vortex. As shown in Fig. 1 there is now a change in the fluid enthalpy when viewed in the absolute frame, as one moves across the x axis.

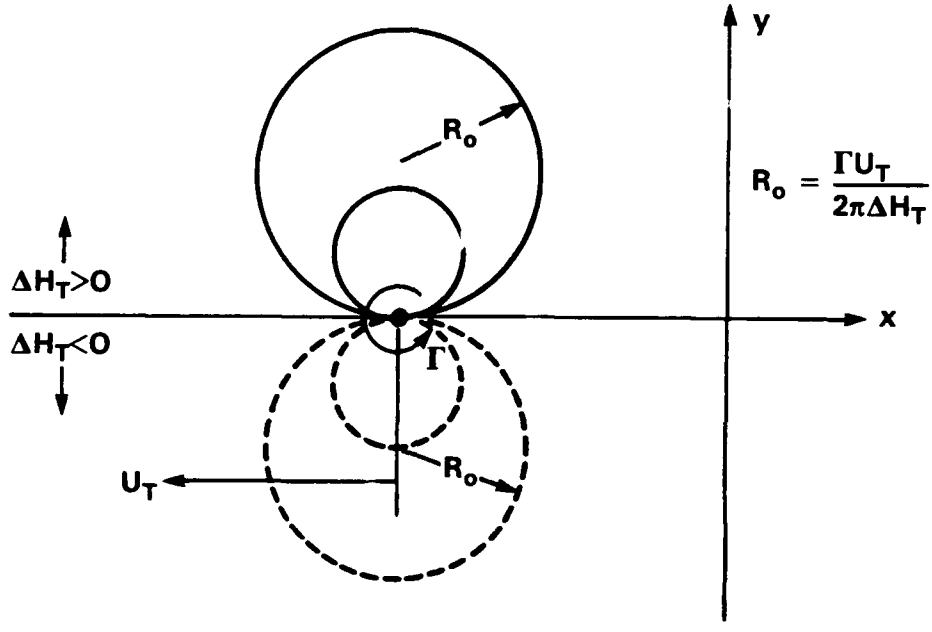

Fig. 1. Contours of constant total enthalpy for a moving vortex.

For a simple two-dimensional turbomachine there is also flow across the vortex, which can be described by additional velocity potentials in both the positive x and y directions:

$$\phi_F = U_x x + U_y y \quad (8)$$

Looking at the vortex center, in a frame of reference attached to the vortex, there is thus a relative velocity.

$$\vec{V}_{rel} = \vec{i}(U_x + U_T) + \vec{j}U_y \quad (9)$$

If one computes the change in the convection of fluid momentum across planes normal to the direction of the relative velocity and at equal distances in front of and behind the vortex position, the result is the force applied to the fluid by the vortex as indicated in Fig. 2.

$$\vec{F}_{N_{rel}} = \int\int \nu_{N_{rel}} \rho_o |V_{rel}| \, d\vec{A} = \rho_o V_{rel} h \int_{-\infty}^{\infty} (\nu_{N_{rel+}} - \nu_{N_{rel-}}) d\vec{n} \quad (10)$$

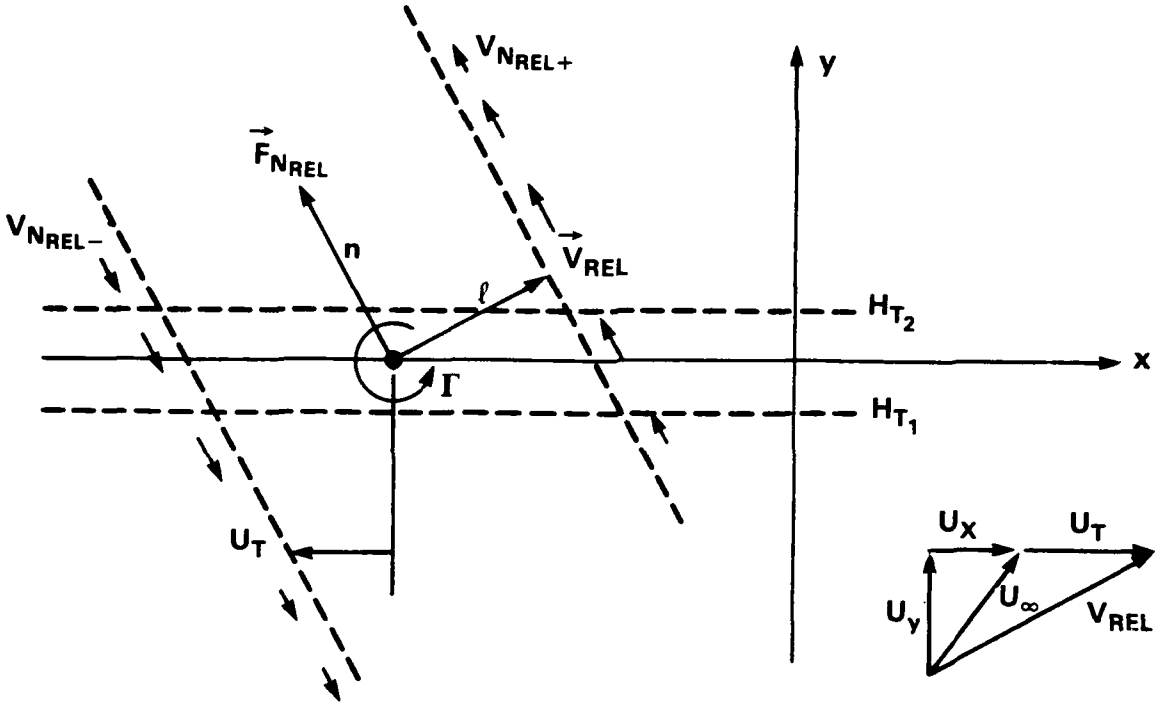

Fig. 2. Boundaries of integration for computing force and work produced by a moving vortex.

Here;

$$v_{N_{rel}} = \frac{\partial \phi}{\partial n} = \frac{\Gamma}{2\pi} \frac{\partial}{\partial n} \tan^{-1} \frac{n}{l} = \frac{\Gamma}{2\pi} \left(\frac{l}{l^2 + n^2} \right) \tag{11}$$

so that:

$$\vec{F}_{N_{rel}} = \varrho_o \Gamma \, V_{rel} \, h \, \vec{n}_{rel} \tag{12}$$

Since forces are independent of the frame of reference, Eq. (12) is also correct for the absolute frame. If now there is a component of this force aligned with the motion U_T, then there must be work input from the surroundings to the flow field. This work force is

$$F_x = F_{N_{rel}} \left(\frac{U_y}{V_{rel}} \right) \tag{13}$$

The time rate of work to the moving vortex i.e., the power, is therefore:

$$P_{IN} = F_x U_T \tag{14}$$

Examining the total fluid field, it is seen that there is convection of mass perpendicular to the direction of vortex motion by U_y. If we compute the increase in energy of the mass flow between any two planes on either side of the x axis, the result is, using Eq. (5);

$$P_{IN} = \int_{-\infty}^{\infty} \varrho_o U_y h(H_{T_2} - H_{T_1})dx = \varrho_o U_y h \frac{\Gamma U_T}{2\pi} \int_{-\infty}^{\infty} \left\{ \frac{y}{x^2+y^2} + \frac{y}{x^2+y^2} \right\} dx \tag{15}$$

$$P_{IN} = \varrho_o U_y h \Gamma U_T = \varrho_o \Gamma V_{rel} h \left(\frac{U_y}{V_{rel}} \right) U_T = F_x U_T \tag{16}$$

Hence the unsteady vortex mathematics is consistent in that the power introduced into the fluid by the moving vortex is represented exactly by the rise in total enthalpy of the fluid convected across the path of the vortex. Thus the solution for the moving single vortex simulates the effect on the fluid of a moving airfoil at some angle of attack.

The global *energy* change, after some time, will appear in the wake of the vortex around a line defined by the relative velocity. The reason for this wake development is associated with the very important fact that in this potential flow there is also a requirement to conserve vorticity. Therefore the instant that the work vortex is initiated a second vortex of equal strength, but of opposite direction, is created simultaneously. This second vortex is convected with the flow, but does not contribute to any further work input since it has no force on it. However, as shown by Wu, the velocity potential of a vortex pair is equivalent to a line of uniform volume dipoles stretched between. Thus the time behavior of this line dipole accounts for the energy change in the wake. Figure 3 illustrates the 2–D streamlines for this situation.

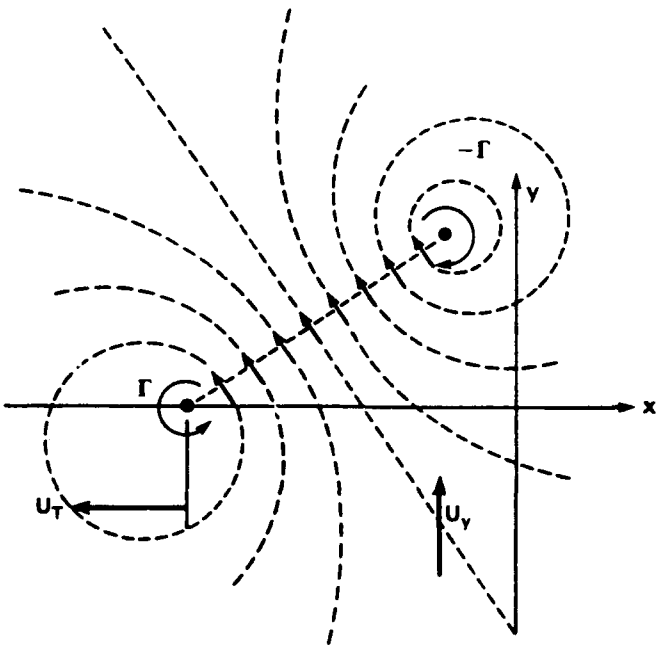

Fig. 3. Vortex pair/dipole equivalence.

A ROW OF MOVING 2–D VORTICES

The previous analysis suggested how a single vortex interacts with a fluid to exchange energy in a two-dimensional flow. This approach has been generalized to an infinite row of two-dimensional vortices, and to a circular arrangement of vortices, by Preston. These two-dimensional geometries simulate the action of axial flow and centrifugal flow turbomachines respectively. Taking for example the infinite row of vortices of strength Γ and separation a, Preston adapts a steady solution for the velocity potential from Lamb.

$$\phi = -\frac{\Gamma}{2\pi} \tan^{-1}\left(\cot\frac{\pi x}{a} \tanh \frac{\pi y}{a}\right) \tag{17}$$

If this vortex row now moves to the –x direction at velocity U_T, then for some x_o in the absolute frame, $x = x_o + U_T t$, and the potential becomes a function time. Taking the space or time derivatives, there results for any point in the flow field, with a superimposed flow:

$$\frac{\partial \phi}{\partial x_o} = u = U_x - \frac{\Gamma}{2a}\left[\frac{\sinh(2\pi y/a)}{\cosh(2\pi y/a) - \cos(2\pi x/a)}\right] \tag{18a}$$

$$\frac{\partial \phi}{\partial y} = v = U_y + \frac{\Gamma}{2a}\left[\frac{\sin(2\pi x_o/a)}{\cosh(2\pi y/a) - \cos(2\pi x/a)}\right] \tag{18b}$$

$$\Delta\frac{\partial \phi}{\partial t} = -\Delta(H_T) = \frac{\Gamma U_T}{2a}\left[\frac{\sin(2\pi x_o/a)}{\cosh(2\pi y/a - \cos(2\pi x_o + U_T t)/a}\right] \tag{18c}$$

Looking on either side of the x axis gives the following asymptotic values for the total enthalpy:

$$H_T(y < a) = \frac{\Gamma U_T}{2a} = U_T u_+ \tag{19a}$$

$$H_T\ (y < -a) = \frac{-\Gamma U_T}{2a} = U_T u_- \ . \tag{19b}$$

Therefore the change in enthalpy of a fluid particle as it moves across the row of translating vortices is $U_T\ \Gamma/a$ or $U_T\ (2u_+)$. If the effect of the remote starting vortex row is included, as in Fig. 4, the enthalpy changes are the same, however, the velocity change is zero for y <– a and $2u_+$ for y > a. Although illustrated here for a two-dimensional cartesian geometry, the result for the circular arrangement of vortices is similar. It may be noted that this analysis does not define how the vortex is generated, only that it be associated with a force on the fluid having a component in the direction of the vortex motion. For the potential flow description of a turbomachine it is assumed that each blade is associated with a vortex, or a group of vortices of variable strength, as required to match the blade surface boundary condition. If the vortices do not move they represent a *cascade* of stationary turning blades where the total pressure is constant, but the static pressure may change according to the Bernoulli relation, Eq. (6).

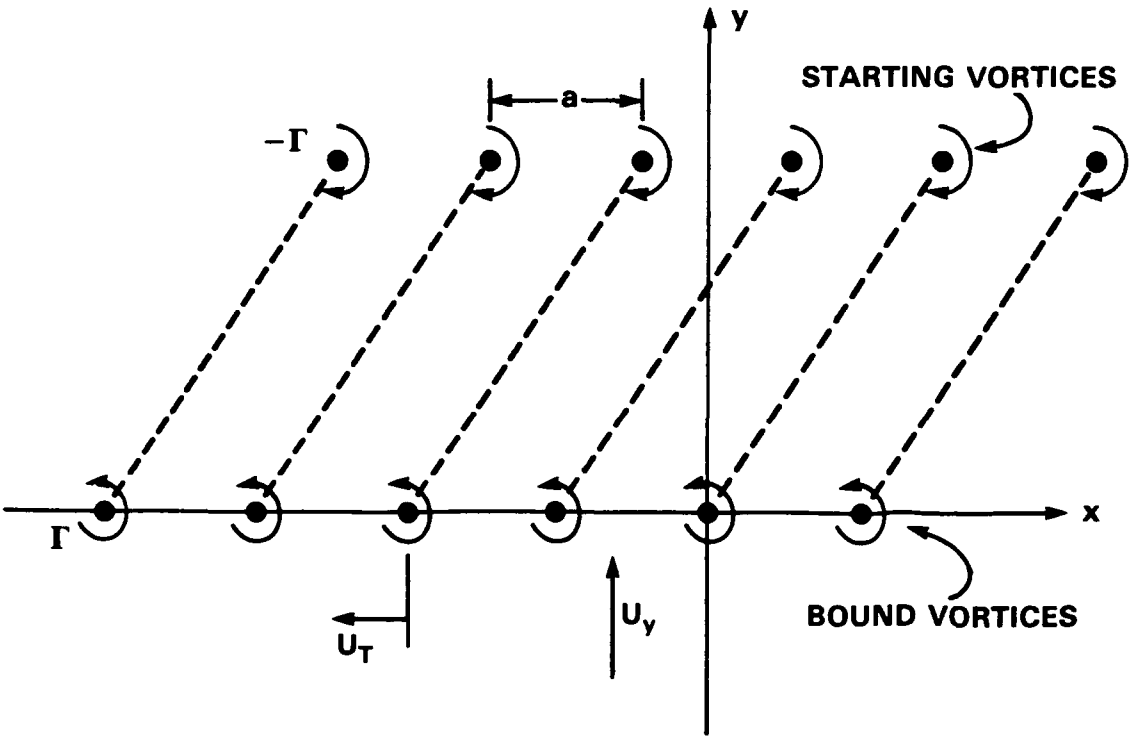

Fig. 4. Bound and starting vortex arrays for a linear blade row.

VORTEX LOOPS AND DIPOLES IN 3–D

For three-dimensional axial flow turbomachinery the vortex velocity potential produces similar effects; however for this case it is necessary to examine more closely the connection between the blade vortex and the starting vortex. In three-dimensions the blade has only a finite span, so the vortex behavior at the root and the tip ends must be accounted for. This is accomplished by introducing two "shed" vortex lines from the ends of a uniformly loaded blade, each having the same strength and continuity of rotation as the blade vortex. These shed vortex lines are convected with the flow through the machine and eventually connect with the starting vortex. Thus in three-dimensions the basic turbomachine vortex system becomes 1) a line vortex along the blade span, 2) two line vortices convecting downstream from the hub and tip, and 3) a starting vortex in the far downstream region. As shown in Fig. 5, this complete vortex system, trailing in a spiral path from the blade disc, will describe all the pressure, velocity and enthalpy changes introduced by the blade. The essential features of the vortex loop trailing from each blade are constant strength, and, area increasing at a constant rate as the blade rotates. Considering the situation in the vicinity of the blade row, it is the growth of this vortex loop that is critical to the work. In the downstream flow, the mathematical combination of all the spiralling vortex loops from many blades creates in the fluid a region of increased enthalpy that has been acted on by the blade row, and outside of this affected region there are no changes.

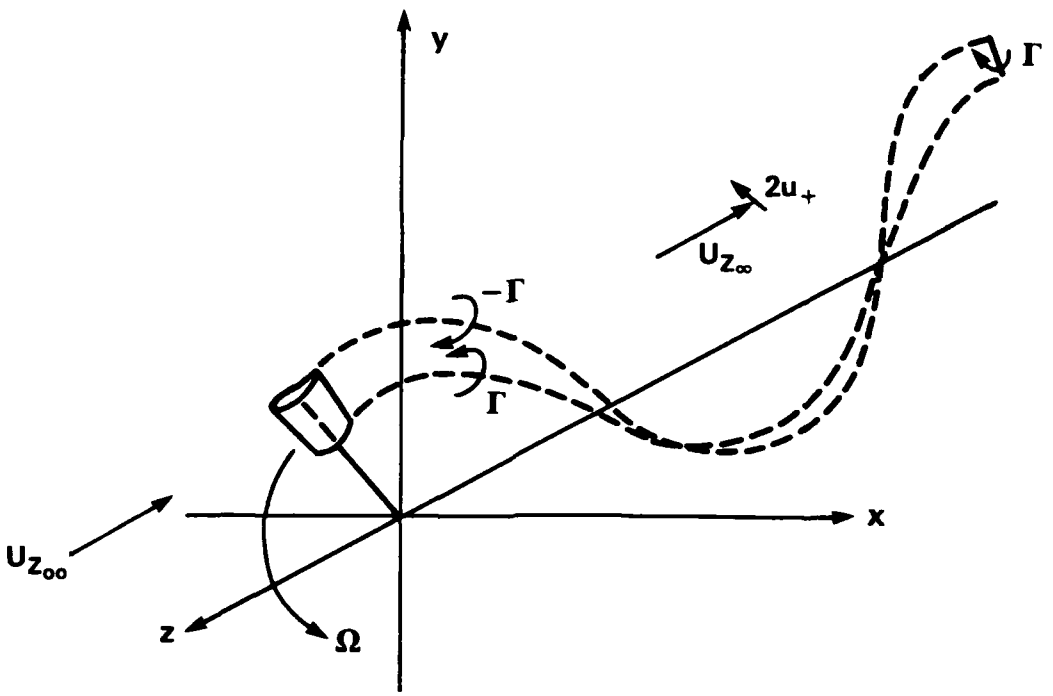

Fig. 5. Three dimensional helical vortex loop created by a rotating blade in axial flow.

Turning to the fluid field near each blade, it can be seen that the vortex loop composed of the blade vortex and the tip and root shed vortices is increasing in area at the rate:

$$\frac{dA_{VL}}{dt} = hV_{rel} \tag{20}$$

Now, Lamb shows that a vortex loop of area A and strength Γ in an undisturbed flow is equivalent to the impulse that was necessary to start that loop in motion.

$$\vec{I}_{VL} = \varrho_o \Gamma A_{VL} \vec{n}_A = \int \vec{F}_{VL} dt \tag{21a}$$

A steady increase of vortex loop area is then equivalent to a steady force applied to the fluid such that

$$\vec{F}_{VL} = \varrho_o \vec{\Gamma} \times \vec{V}_{rel} h \tag{21b}$$

which is the three-dimensional equivalent of Eq. (12). Furthermore, the steady velocity potential at any remote point due to an incremental area of vortex loop at the origin is given by Lamb as

$$\phi_{VL} = \frac{\Gamma}{4\pi} \vec{n}_o \cdot \vec{n}_a \frac{\Delta A_{VL}}{r_o^2} \tag{22}$$

where n_o is the vector from the origin to the field point and r_o is the distance. The form of (22) is such that it is equal to the velocity potential of a steady volume dipole located at the area centroid, and having a direction normal to the plane of the vortex loop area as illustrated in Fig. 6, and given by (23).

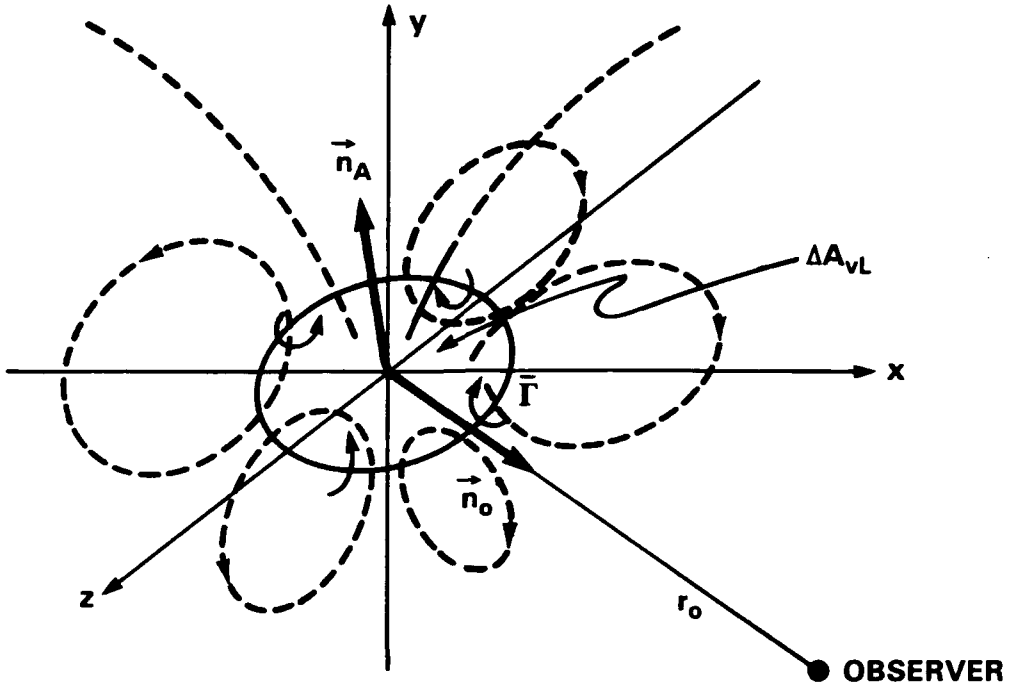

Fig. 6. Coordinate definitions for the velocity potential of a three-dimensional vortex loop.

$$\phi_D(r_D,\beta) = \frac{\Delta D_v}{4\pi r_o^2}\vec{n}_o \cdot \vec{n}_D \tag{23}$$

Thus the incremental dipole strength is equivalent to $\Gamma\Delta A$, and it can be seen that continuous expansion of vortex loop area is equal to continuous injection of dipoles into the flow field from the position of each blade. In fact, the DNA-like spiralling double helix of the vortex pair shed into the wake of each blade can be replaced mathematically with a single helical line dipole centered between the vortex pair. From an equivalence standpoint it is possible to say all of the following:

$$\vec{F}_v = \frac{d\vec{\Gamma}_v}{dt} = \varrho_o\vec{\Gamma}\mathrm{x}\vec{V}_{rel}h = \varrho_o\vec{\Gamma}\mathrm{x}\frac{d\vec{A}_{VL}}{dt} = \varrho_o\frac{d\vec{D}_v}{dt} = \varrho_o V_{rel}\frac{d\vec{D}_v}{ds} \tag{24}$$

DIPOLE COMPONENTS FROM GREEN'S THEOREM

In addition to the work done by a blade as it moves, the fact that each blade has a finite volume means that fluid must be displaced continuously from the front and pulled

into the back as the blade moves. The potential flow solution for the case of a rigid body moving through a fluid is presented fully by Lamb. However, recently, Lighthill has presented a more physically significant approach to this situation. Following Lighthill, the Green's surface integral theorem allows a velocity potential at any position in a flow field to be computed from two integrals of the originating potential over the surface of the body creating the flow. When the point p is geometrically remote from the body;

$$\phi_{(p)} = \frac{\vec{n}_o \cdot}{4\pi r_o^2}\left[\int\int \phi \vec{n}_s ds - \int\int \vec{s}\frac{\partial \phi}{\partial n} ds\right] \tag{25}$$

Evaluation of these integrals for the case of a general body shape shows that

$$\int\int \phi \vec{n}_s \, ds = \vec{G}_1 = \vec{I}/\varrho_o \tag{26a}$$

$$\int\int \vec{s}\frac{\partial \phi}{\partial n} \, ds = \vec{G}_2 = \Delta \vec{U} \tag{26b}$$

where $\vec{I}$ is the impulse applied to the fluid external to the body to establish that flow field, and Δ is the volume of fluid displaced by the body. In addition to the above effects of rigid body motion, Lighthill shows that if there is a circulation, Γ, associated with the body, as is the case for the lifting airfoil, then there must be a three-dimensional vortex system in the region, and that the lift force in particular is given by the time rate of change of the volume integral of the vector moment of vorticity over the entire region:

$$\vec{F}_L = \frac{\varrho_o}{2}\frac{\partial}{\partial t}\int\int\int (\vec{x} \times \vec{\zeta}) \, d\forall \tag{27a}$$

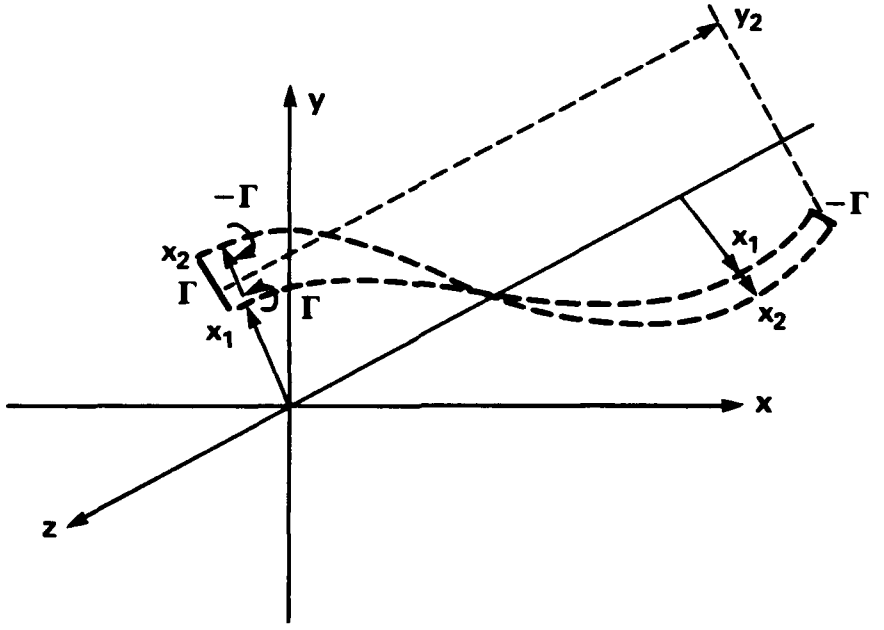

Fig. 7. Coordinate system for evaluation of vorticity moment volume integral.

Here the integral must be taken over all space so as to include the whole vortex loop. Of course in potential flow the bulk vorticity is zero, but in singular regions, where the vortex lines exist, one can say:

$$\int\int \zeta dA = \Gamma n_v \tag{27b}$$

so that the integral of (27a) gives the force of (24). Now, as Lighthill points out, it just so happens that the impulse term of (26a) can be related, through a theorem by Kelvin, to a system of vortex loops placed in the surface of the body to account for the tangential slip velocity. If then these vortex loops are used to describe the impulse term, Lighthill obtains the simple, but acoustically useful, result for the total force to move a blade body through a fluid.

$$\vec{F}_{(t)} = \frac{\varrho_o}{2}\frac{\partial}{\partial t}\int\int\int (\vec{x} \times \vec{\zeta}) d\forall + \varrho_o \Delta \frac{d\vec{U}}{dt} \tag{28}$$

It should be noted that from a large distance all of the surface shear vortex loops can be combined to appear as one dipole. Interestingly, for harmonic motion, the only possible net power input to a non-lifting body is through the surface shear term, so it will be illustrative to study later in more detail the oscillating motion of dipoles. Before examining periodic dipoles however, it is important to discuss the vortex/dipole system associated with centrifugal flow turbomachines.

VORTEX FORMATION IN CENTRIFUGAL ROTORS

The previous models of unsteady potential flow were developed implicitly for linear or axial flow machines where there is little fluid motion in the radial direction. Although it was noted that Preston proved that a rotating ring of vortices simulated correctly the energy transfer in a radial flow geometry, the details were not examined. Therefore, it is appropriate now to look further into the application of vortex loop concepts to more general turbomachines having centrifugal effects.

Before proceeding, the term "unsteady potential flow" deserves some clarification. Examination of Eq. (1) shows that solutions for the velocity potential depend primarily on geometric boundary conditions. Thus these solutions are time-dependent only in the sense that they represent instantaneous velocity fields compatible with a set of instantaneous boundary conditions. Therefore, the computed velocity fields have no "memory". The pressure field is different since, through Eq. (4), it depends on the rate of change of the vector velocity and will affect the solution through any boundary condition related to pressure.

For generallized turbomachines, the standard kinematic boundary condition applied to Eq. (1) is that the *relative* velocity normal to any solid surface, stationary or moving, is zero (i.e., the relative velocity is always tangent to the surface). This condition represents compensation for any local angle of attack on the surface by the undisturbed flow. For airfoil shapes with a sharp trailing edge, the boundary condition at that point, that substitutes for viscosity, is that the pressure be continuous and finite. (e.g., a stagnation point.) In matching this condition with vortex singularities it is necessary to locate vortex lines along the blade, with the shed vortex system convected along relative flow streamlines, such that the flows from opposite sides merge smoothly at the trailing edge.

Since the relative velocity is so critical to a rotating machine, it is common to perform its analysis in a frame of reference that rotates with the shaft. Thus the relative fluid velocity in a frame rotating at speed Ω is given by;

$$\vec{W} = \vec{V} - \vec{\Omega} \times \vec{r} \tag{29a}$$

Because the inviscid flow is assumed to remain irrotational in the absolute frame, i.e., $\zeta = 0$, it is straightforward to show that,

$$\vec{\nabla} \times \vec{W} = -2\vec{\Omega} \tag{29b}$$

and, in general, the relative velocity will be rotational and not subject to a simple potential flow treatment. Nevertheless, W can often be treated as steady, which simplifies the momentum equation. Making the strictly kinematic transformation of the linear momentum equation, (Eq. (4), into a rotating frame yields;

$$o \approx \frac{\partial \vec{W}}{\partial t} = \frac{-1}{\varrho_o}\vec{\nabla}p - \vec{\nabla}(W^2/2) - (\vec{\nabla} \times \vec{W}) \times \vec{W} - \vec{\Omega} \times (\vec{\Omega} \times \vec{r}) + 2\vec{W} \times \vec{\Omega} \tag{30a}$$

Substituting (29b) into (30a) shows that the rotational and Coriolis terms cancel to give

$$o \approx \frac{\partial \vec{W}}{\partial t} = \vec{\nabla}(p/\varrho + W^2/2) - \vec{\Omega} \times (\vec{\Omega} \times \vec{r}) = \vec{\nabla}(Rothalpy) \tag{30b}$$

Equation (30b) is therefore a rather general expression for computing the time-average local pressure in the rotating frame.

If the velocity potential in the absolute frame is such that the relative flow is steady, then it can be seen that the flow field rotates with the blades, and $\phi\ (r, \theta, t)$ becomes $\phi\ (r, \theta - \Omega t)$. Using this form in Eq. (4) gives;

$$\vec{\nabla}\left(\frac{\partial \phi}{\partial t}\right) = -\Omega\vec{\nabla}\left(\frac{\partial \phi}{\partial \theta}\right) = -\vec{\nabla}(U_\theta V_\theta) = -\vec{\nabla}(p/\varrho + V^2/2) = -\vec{\nabla}(H_T) \tag{31}$$

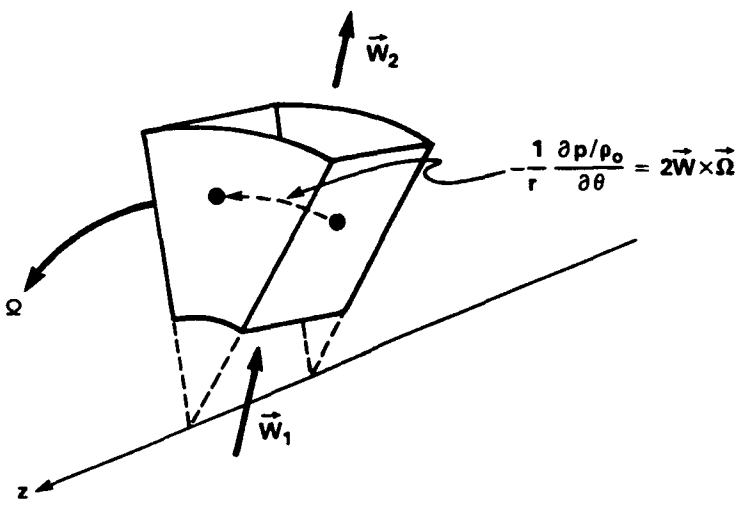

Fig. 8. Illustration of "Coriolis" force in the rotating frame.

and for steady flow in the rotating frame, Eq. (30b) beomes:

$$o = -\vec{\nabla}(p/\varrho + W^2/2 - (\Omega r)^2/2) \; ; \; or \; \vec{\nabla}(H_T) = \vec{\nabla}(V^2/2 + (\Omega r)^2/2 - W^2/2) \quad (32)$$

In either case the mean change in absolute frame total enthalpy is given by the mean change in $U_\theta V_\theta$. This is the Euler 3–D generallization of Eq. (7). If the flow is unsteady in the relative frame, then the relative velocity must be integrated along desired paths at successive instants, and the time rate of change computed in order to obtain a local pressure from (30b).

In applying the vortex singularity model to a purely centrifugal rotor, it should be noticed first of all that there will be some $r-\theta$ blade profile such that the condition of zero relative flow normal to the blade surface is met with no vortex systems required. This "no-lift" blade shape can be seen to have a greater slope as the radius increases due to Eq. (29a). As the blade shape departs from the no-lift profile, bound and shed vortex lines must be introduced to keep the flow tangent to the surface and meet the trailing edge condition. As the blade becomes primarily radial, the bound vortex distribution will be strengthened toward the outer radii because of the higher circumferential velocities to be cancelled. For closely-spaced radial blades, the fluid at mid-radii can experience flow that is mainly radial such that W_θ is small. In this region, since $\zeta = 0$ and the rothalpy is constant throughout, the following approximations apply;

$$|\vec{\nabla} \times \vec{W}| = \frac{1}{r}\frac{\partial r W_\theta}{\partial r} - \frac{1}{r}\frac{\partial W_r}{\partial \theta} = -2\Omega; \; \frac{\partial W_r}{\partial \theta} \approx 2U_\theta \; \& \; \frac{\partial p}{\partial \theta} \approx -2\varrho W_r U_\theta \quad (33)$$

In this example, significant circumferential variations in radial velocity, as well as a Coriolis-like distribution in static pressure occur as illustrated in Fig. 8. Near the trailing edge of the radial blade, relaxation of this pressure gradient into the fluid beyond the rotor creates a flow in the negative W_θ direction. This reduces machine work and sets up the classic "jet-wake" behavior described by Dean and Senoo for centrifugal rotors. Certainly, the overall behavior is described by the system of rotating vortices, which when summed for each blade, act as described by Preston. But, the unique pressure distribution for centrifugal turbomachines causes a non-uniform exit flow field that will be shown later to be acoustically important when it encounters a downstream stator.

ACOUSTICS OF DIPOLES

PROPAGATION OF THE VELOCITY POTENTIAL

For various kinds of turbomachines, the blades, rotating or fixed, have been shown to result in the introduction of vortex loops or equivalently dipoles, into the flow field. For rotating blades, the time-varying velocity potentials from these singularities account for the power transfer to the fluid, while if the blades are stationary the energy level of the fluid is constant and strictly Bernoulli changes occur. Turning to the acoustics, it is now appropriate to ask how these primarily incompressible potential flow effects are transformed into acoustic signals that propagate over large distances. To introduce the acoustic analysis, it will be assumed that the fluid density can in fact experience very small variations with pressure through an isentropic equation of state such that;

$$\delta\varrho = \delta p/c^2 \quad (34)$$

Writing the equations of conservation of mass and momentum for the absolute frame gives

$$\frac{\partial \varrho}{\partial t} + \vec{\nabla} \cdot \varrho \vec{V} = o \tag{35}$$

$$\frac{\partial \vec{V}}{\partial t} = -\frac{1}{\varrho}\vec{\nabla}(p + \varrho V^2/2) \approx -\frac{1}{\varrho_o}\vec{\nabla}p \tag{36}$$

Here, following Lamb, the kinetic energy part of the total pressure can often be neglected for acoustic purposes. Using (34) in (36) and integrating in time gives a relationship between velocity and density perturbations.

$$\vec{V} = \vec{\nabla}\phi = -\vec{\nabla}\int p/\varrho_o dt = -\vec{\nabla}\int c^2 \delta\varrho/\varrho_o dt \tag{37}$$

Using this result in Eq. (35), with the condition that $|V/c|$, the local Mach number, is small gives

$$\nabla^2\phi - \frac{1}{c^2}\frac{\partial^2\phi}{\partial t^2} = o \tag{38}$$

Equation (38) is the basic wave equation having solutions made up of functions that propagate in space at velocity c. Using the same approach it is possible to show that other variables such as p, V *or* $\delta\varrho$ will also propagate as functions delayed by the time $\tau = x/c$.

DEFINITION OF DIPOLE-IMPULSE ACOUSTICS

For acoustic analysis it is often convenient to locate any unsteady activity near the origin of the coordinate system and to determine the value of the propagating function at some remote observation point. For a three-dimensional spherical geometry, with a volume source at the origin, it is straight forward to show that the product ϕr will propagate radially outward from the origin with constant amplitude. The velocity potential for the dipole is constructed, therefore, by combining the solutions for two time-varying volume sources of opposite sign, located near the origin, and separated by a small distance, 2a, along some time-varying direction vector, n_D. If the strength of the dipole is defined as

$$D(t) = \underset{a \to o}{Lim} \left[2aQ(t)\right] \tag{39}$$

then the velocity potential at any point in the field of Fig. 9 is given by Eq. (40) which includes behavior both near and far from the origin.

$$\phi_D(r,t) = -\vec{n}_o \cdot \left[\left(\frac{D(t)}{4\pi r^2} + \frac{D'(t)}{4\pi r c}\right)\vec{n}_D(t)\right]_{t-r/c} \tag{40}$$

Looking at the ϕr product it can be seen that the grouping

$$\phi_{Da}r = -\vec{n}_o \cdot \left[\frac{D'(t)}{4\pi c} \vec{n}_D(t) \right]_{t-r/c} \tag{41}$$

will propagate to large distances unattenuated. As is conventional in acoustic terminology, the square brackets indicate that the function inside is to be evaluated at the retarded time.

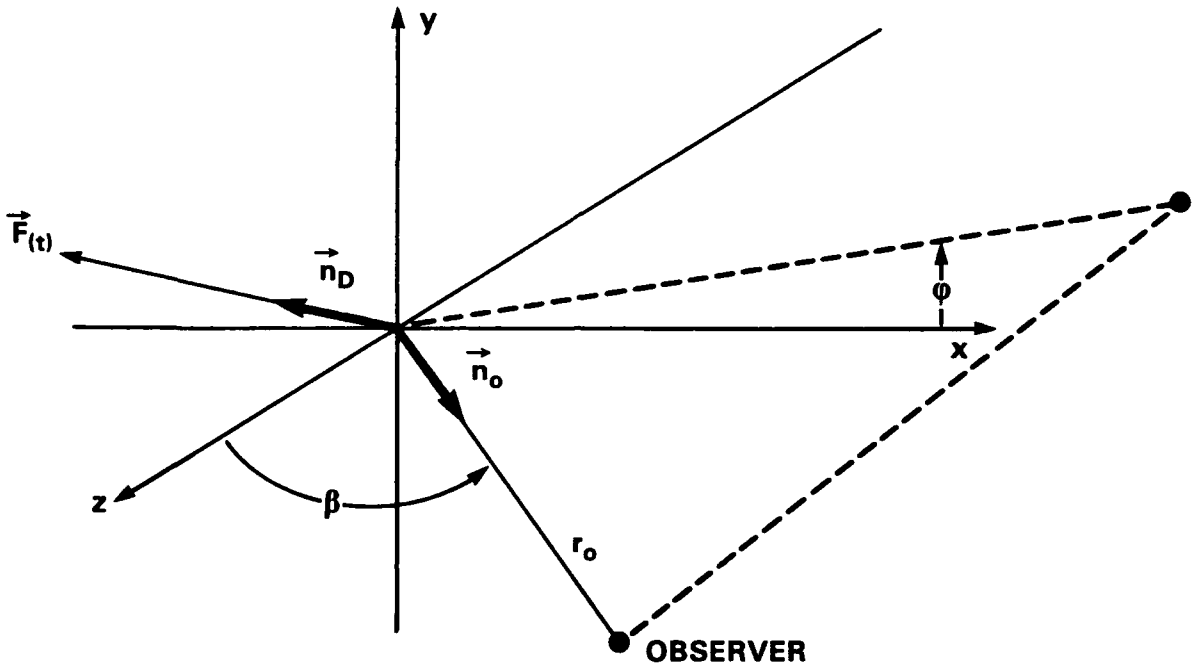

Fig. 9. Geometry for dipole radiation.

Therefore the acoustic velocity potential, and all the other far–field properties that can be derived from it, depends on the *time derivative* of the source strength. Using the equivalencies of Eq. (25) it can be seen that for a dipole that simulates a vortex loop,

$$p_{va}(r,t) = -\varrho_o \frac{\partial \phi_{va}}{\partial t} = \frac{\vec{n}_o \cdot}{4\pi r c} \left[\frac{\partial \vec{F}_v}{\partial t} \right]_{t-r/c} \tag{42a}$$

and for the more general case described by Lighthill in Eq. (28) for a body moving in a fluid, the acoustic pressure is;

$$p_a(r,t) = \frac{\vec{n}_o \cdot}{4\pi r c} \left[\frac{\partial \vec{F}}{\partial t} \right]_{t-r/c} \tag{42b}$$

Equations (42) are the ubiquitous acoustic results for the application of a force to a small fluid region. For a turbomachine with multiple blades, the acoustic pressure from each source is summed to obtain the value at any observation point. Although the procedure of

applying Eq. (42) appears simple, it is in fact difficult because of the critical importance of the time delay operation when summing signals that originate from different parts of the flow. Before proceeding with techniques for the evaluation of Eq. (42) for turbomachinery, it will be revealing to examine first the simple classic case of dipole acoustics

VELOCITY POTENTIAL FOR THE OSCILLATING SPHERE

As developed previously, the dipole is related to the vortex loop, and to the impulse that creates such a flow. In addition, the dipole singularity can represent other effects such as the flow field associated with the motion of a rigid sphere or the pressure on a surface caused by a time-varying force within the surface. Considering only the sphere, there are several cases of acoustic interest, e.g.;

- Stationary sphere in a time-varying flow
- Moving sphere in a stationary fluid
- Sphere oscillating at a small amplitude
- Sphere rotating in a plane about the origin

In each case it is necessary to compute the remote acoustic velocity potential from some local boundary conditions near the origin. In general, this problem in potential flow is handled using the Green's integral method, including the time delay operation. Thus, if the potential is known on some surface in a three-dimensional flow field, the potential at some remote point is;

$$\phi_p(\vec{r},t) = -\frac{1}{4\pi}\int\int \frac{1}{r}\left[\frac{\partial\phi}{\partial n}\right]_{t-r/c} ds + \frac{1}{4\pi}\int\int \frac{\partial}{\partial n}\left(\frac{\phi(t-r/c)}{r}\right) ds \qquad (43)$$

where in the second integral only the time delay part of the surface derivative is used.This equation is generally difficult to evaluate, except in simple cases where the surface potential is known. One of those cases that will serve as an example is that of the rigid sphere oscillating in a fixed direction at small amplitude, as shown in Fig. 10. For this case a dipole potential can be defined easily and far-field solutions obtained. To do this it is first assumed that the scalar dipole strength can be described as a periodic function that is independent of direction.

$$D(t) = D_o(j\omega)e^{j\omega t} \qquad (44)$$

This must satisfy the boundary condition at the rigid surface that:

$$u_r(r,\beta,t) = \frac{\partial\phi}{\partial r}\Big|_{r=R} = U_{z_o}e^{j\omega t}\cos\beta \qquad (45)$$

Since for any observation point, $\vec{n}_D \cdot \vec{n}_o = \cos\beta$, it is possible to combine Eqs. (40), (44) and (45) to obtain an expression for $D_o(j\omega)$.

$$D_o(j\omega) = 2\pi R^3 U_{z_o}\frac{(1-(kR)^2/2-jkR)}{((1-kR)^2/2)^2+(kR)^2} \qquad (46)$$

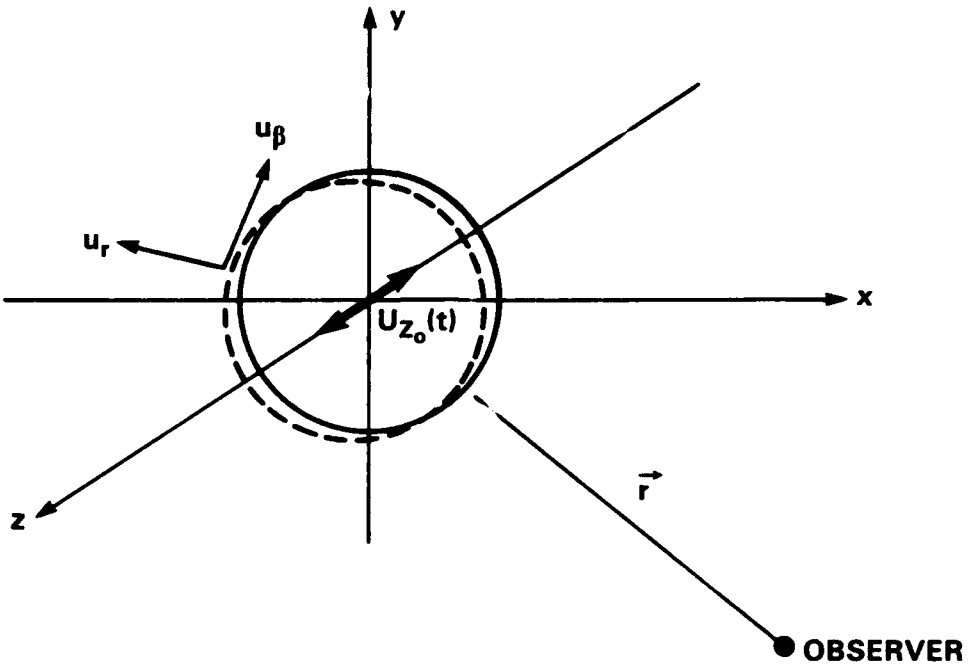

Fig. 10. Sphere oscillating at small amplitude in Z direction.

Here $k = \omega/c = 2\pi/\lambda$ and it is generally assumed that the acoustic wavelength will greatly exceed the sphere circumference, i.e., $kR \ll 1$. Thus for this case the complete velocity potential is:

$$\phi(r,t) = -\left\{ \frac{D_o(j\omega)}{4\pi r^2} + \frac{j\omega D_o(j\omega)}{4\pi r c} \right\} \cos\beta \; e^{j\omega(t-r/c)} \tag{47}$$

Putting (47) into (43), where the surface of integration is chosen to be that of the sphere, gives for the far field; (here, $r = r_o - Rn_o \cdot n_s$, and only the near field part of (47) is used)

$$\phi_a(r,t) = -\frac{\cos\beta}{4\pi r_o c}\left[\Delta \frac{dU_z}{dt} + \frac{\Delta}{2}\frac{dU_z}{dt} \right]_{t-r/c} \tag{48}$$

Thus the acoustic velocity potential is composed of two terms, one depending on the acceleration of the displaced volume and the other on the acceleration of half the displaced volume, or the "added" volume. This result is general and is obtained in the same way for any propagating scalar. Although (48) could have come from (46) and (47), the use of (43) provides the acoustic parallel to Eq. (25), and the analogy between (28) and (48).

POWER INPUT TO THE OSCILLATING SPHERE

Having Eq. (47), it is of interest from the energy viewpoint to examine the power flow. Since no work is done, other than acoustic radiation, this will give some insight into the source of the acoustic power alone. Looking at the sphere itself, the time-average power input is determined from the product of force and velocity in the z direction.

$$P_{IN} = \frac{1}{2} \text{ Re } \left[F_z(j\omega) \cdot U_z^* \ (j\omega)\right] \tag{49}$$

The time-varying force in the z direction is found by integrating the static pressure over the surface of the sphere.

$$F_z(t) = \int_o^\pi p(R,\beta,t)\cos\beta \ 2\pi \ R\sin\beta \ R \ d \ \beta \tag{50}$$

From Eq. (5) the static pressure is;

$$p(r,\beta,t) = -\varrho_o \frac{\partial \phi}{\partial t}\Big|_{r=R} - \varrho_o(u_r^2 + u_\beta^2)_{r=R} \tag{51}$$

The component surface velocities can be computed from (47) as

$$u_r = \frac{\partial \phi}{\partial r}\Big|_{r=R} = U_{z_o}\cos\beta e^{j\omega t} \quad ; \quad u_\beta = \frac{1}{r}\frac{\partial \phi}{\partial \zeta}\Big|_{r=R} = -\frac{\phi(R,t)}{R}\tan\beta \tag{52}$$

It can be seen that the angular dependencies of the kinetic energy terms are such that when used in (50) the result will be zero. Thus the z direction force becomes only a function of the first term in (51).

$$F_z(t) = \int_o^\pi \varrho_o D_o(j\omega) j\omega \left(\frac{1}{4\pi R^2} + \frac{j\omega}{4\pi R c}\right) e^{j\omega(t-R/c)}\cos^2\beta \ 2\pi \ R^2 \sin\beta d\beta \tag{53}$$

The complex value of the integral, using (46) for $D_o(j\omega)$, and assuming kR is small, is

$$F_z(j\omega) = \varrho_o \frac{\Delta}{2} U_{z_o}\omega(j + (kR)^3/2) \tag{54}$$

Equation (54) shows that there is an inertial force on the sphere associated with the added volume, $\Delta/2$ with a small fraction of that force being in-phase with velocity. Therefore from (49) the mean power input needed to oscillate the sphere is:

$$P_{IN} = \left(\varrho_o \frac{\Delta}{2} U_{z_o} \ \omega\right) \frac{U_{z_o}}{2} \cdot \frac{(kR)^3}{2} \tag{55}$$

POWER PROPAGATING FROM SPHERE

To obtain this result from a different view, one can also compute the acoustic power that radiates to infinity from the origin. Thus in the far field;

$$p_a(r,t) = -\varrho_o \frac{\partial \phi}{\partial t} = \frac{-\varrho_o j\omega D_o(j\omega)\ j\omega\ e^{j\omega(t-r/c)}}{4\pi r\ c} \cos\beta \qquad (56a)$$

$$u_a(r,t) = -\varrho_o \frac{\partial \phi}{\partial r} = \frac{-j\omega D_o(j\omega)\ j\omega\ e^{j\omega(t-r/c)}}{4\pi r\ c^2} \cos\beta \qquad (56b)$$

It can be seen that $p_a = \varrho_o c u_a$, as in plane wave propagation, and for $kR << 1$ both coefficients are real and in-phase. Their product gives the time average acoustic intensity.

$$I_a(r_o,\beta) = \frac{\varrho_o \omega\ D_o^2 k^3}{2(4\pi r_o)^2} \cos^2\beta \qquad (57)$$

Integrating this over an arbitrarily large spherical surface, with $D_o = 2\pi R^3 U z_o$ gives;

$$P_{OUT} = \frac{1}{2}\left(\frac{4\pi R^3}{3}\varrho_o\right) U_{z_o}\omega \left(\frac{U_{z_o}}{2}\right)\frac{(kr)^3}{2} \qquad (58)$$

Which is exactly equal to the input power, Eq. (55). Looking at (56a) more closely,

$$p_a(r_o,\beta) = 3\left(\frac{\varrho_o \Delta}{2}\right)\frac{U_{z_o}\omega \cdot \omega}{4\pi r_o c} \cos\beta \qquad (59)$$

which suggests from Eq. (42b) that the force involved in creating the acoustic signal is *proportional to* the inertial acceleration of the added mass *and* the displaced mass terms. Thus the total apparent force *experienced by the fluid* is found by considering the inside of the sphere as being filled with the surrounding fluid. This is consistent with Lighthill's expression for the total force, Eq. (28), and the general solution, Eq. (48). However, now it can be seen, by comparing (28) and (48), that the time derivative of the volume integral of the vorticity moment must be equal to the acceleration of the *added mass*. This is in fact the case because the displaced mass effect is associated with the radial velocity of the sphere while the added mass is associated with the tangential velocity on the sphere. The latter effect is equivalent to a set of vortex loops in the surface of the sphere that account for the slip on this surface. The combined effect of this set of ring vortices is one single vortex loop with its axis in the z direction. In the far-field this vortex loop appears as a single dipole representing the effect of the added mass. Through Eq. (54), this added mass dipole includes a small component in-phase with the velocity, and therefore accounts for all the acoustic power input.

To summarize the acoustic behavior of the oscillating sphere, the total force acting on the fluid as a result of the motion, and which is the apparent source of radiation into the far field, is due to the inertia of both the "displaced" and "added" masses. Interestingly, the displaced mass term cannot contribute to the acoustic power since its force is always in quadrature with the velocity. However, it so happens that the added mass term contains a small component in phase with velocity, which accounts fully for the acoustic power. In addition, the added mass term is related to a distribution of vortex rings on the surface of the sphere, and thus to a single dipole, and finally to the impulse needed to set up an external tangential flow around the sphere. Thus, although it can be seen from Eq.

(40) that the tangential velocity itself does not propagate to the far-field, the impulse responsible for it does. More to the point, this particular vortex ring result is related to the vortex loops introduced by the work input action of turbomachine blades. Thus, In the case of the work vortices, only Eq. (42a) is necessary if the blade volume is negligible. Finally, when extrapolating from the near field to the far field it is important to realize that there are two components to Eqs. (28) or (43). One author, Blake, used only the radial surface velocity to compute far field pressure, and obtained two-thirds of the answer. The use of a scalar function instead of a vector to extrapolate to the far–field will prevent this type of error.

ACOUSTIC INTERFERENCE FOR TURBOMACHINES

Turbomachines represent a unique case in the computation of the far-field sound pressure from Eq. (42) because the dipole sources are, by definition, located in a circular pattern about the rotational axis. If the sources are the steady work forces that the rotor blades apply to the fluid, then they simply rotate in space at constant amplitude. On the other hand if the acoustic sources are the dynamic forces on stator blades, perhaps due to the wake of an upstream rotor, then the sources are stationary in space, while the exitation pattern rotates. In all cases the common requirement for solving Eq. (42) is to determine how time delays can be accounted for with a circular array of sources. To illustrate the approach to this problem for low Mach number applications, two basic acoustic propagation geometries will be examined for steady shaft rotation about a point fixed in space;

- Radiation into a free-field
- Radiation in a cylindrical duct

For each case the solution will be examined for a rotor alone, for a stator behind a rotor, and for a rotor operating in a spatially non-uniform inflow. In cases where the flow exitation is periodic, the force response will be assumed to be linear in the perturbed flow. For an isolated blade or a cascade, the appropriate Sears function will give the unsteady force for the airfoil, while the "Coriolis" force must be used for rotors with radial flow conditions. It will also be assumed that the effects of finite blade volume can be described by the potential source functions described previously for the solid sphere as in Quandt.

FREE-FIELD

Gutin Sound From a Rotor

This case, representing a stationary open propeller, was first analyzed correctly by Gutin, and the result is termed "Gutin Sound". Because the solution is basic to all later analyses, the approach will be described in some detail. For steady inflow to a single propeller blade, the work force is seen to be constant in magnitude, but varying in direction and point of origin as the blade rotates. Since this problem is symmetric about the z axis of rotation, it is convenient to locate the observer in the $x-z$ plane, as shown in Fig. 11. Thus the blade force vector becomes

$$\vec{F} = | F | \vec{n}_s = F(-\vec{i} \sin\gamma \ \sin\theta_s + \vec{j} \sin\gamma \cos\theta_s - \vec{k} \cos \gamma) \qquad (60)$$

where γ is the angle between the blade zero lift line and the x axis. The unit vector to the observer's position is;

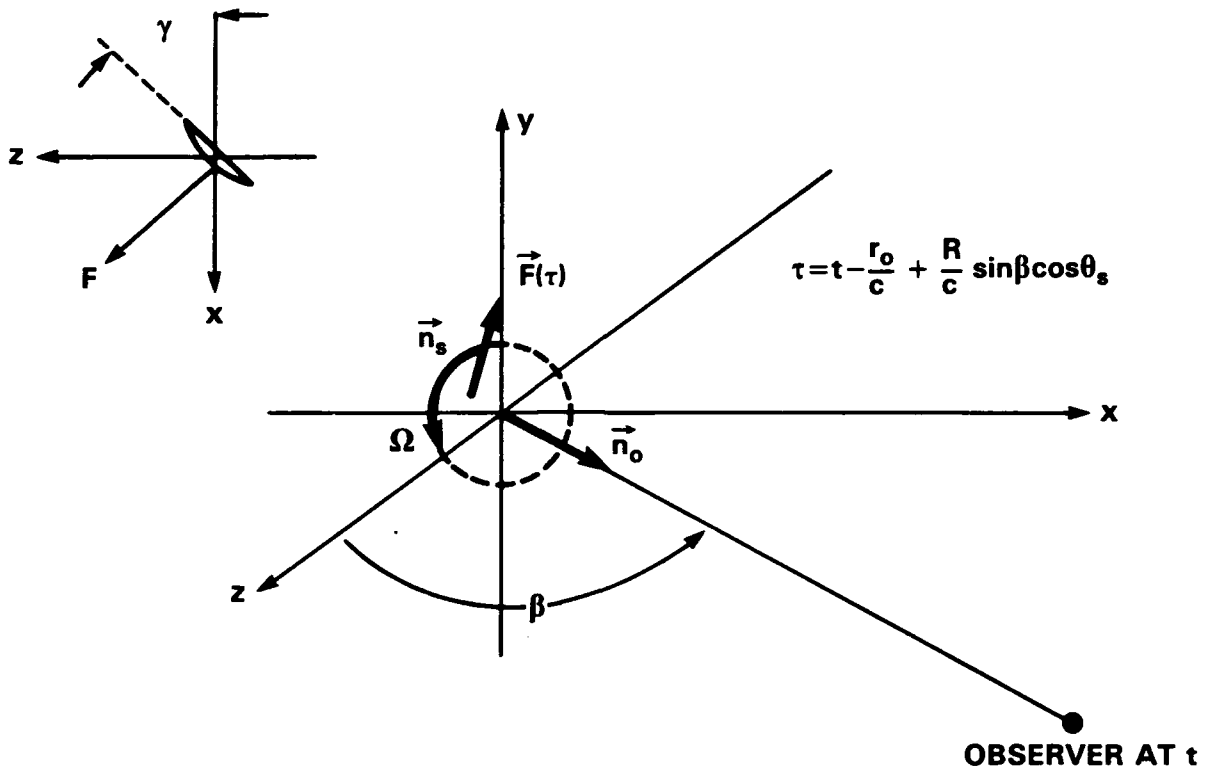

Fig. 11. Acoustic geometry for a single blade rotating in the x-y plane.

$$\vec{n}_o = \vec{i}\sin\beta\cos\psi + \vec{k}\cos\beta \tag{61}$$

and the function that the observer in the +x hemisphere ($\psi = 0$) will see is:

$$\frac{\partial}{\partial t}\left[\vec{n}_o \cdot \vec{F}\right]_{t-r/c} = \frac{\partial}{\partial t}\left[-F\sin\gamma\sin\beta\sin\theta_s + F\cos\gamma\cos\beta\right]_{t-r/c} \tag{62}$$

In Eq. (62) the second term represents an axial force that is steady in time and direction, but varying in origin as the blade rotates. It's time derivative gives rise to a term that is linear in Mach number, and thus it will be neglected at this point. The first term is more clearly time dependent since $\theta_s = \Omega\ t$. It represents the torque force on the blade, and as such can be seen to have force components that oscillate in the x and y axes. (It may be noted that the observer in the $x-z$ plane will see no variation in signal from the component along the y direction).

With a force that repeats periodically at frequency Ω, it can be assumed that the observer will also experience an acoustic pressure from Eq. (42) that is periodic at Ω, such that;

$$p_a(r,\beta,t) = \sum_{n=-\infty}^{\infty} A_n(r,\beta)\ e^{jn\Omega t} \tag{63}$$

and it is desired to determine the A_n terms. Now, any signal reaching the observer at time t had to originate at some earlier time. By the geometry of the system, the distance from a blade-fixed source rotating at some radius about the origin, to the chosen far field observer is:

$$r = r_o\left(1 - \frac{R}{r_o}\ \sin\beta\ \cos\theta_s\right) \tag{64}$$

Therefore the angular position of the blade at an earlier time, determined by the acoustic delay, at which a signal originated that reaches the observer at t is:

$$[\theta_s] = \Omega\left(t - r_o/c + \frac{R\sin\beta}{c}[\theta_s]\right) + \theta_{so} \tag{65}$$

Solving Eq. (65) for $n\ \Omega\ t$ and substituting in Eq. (63) gives;

$$n\Omega t = n\left\{[\theta_s] + \frac{\Omega r_o}{c} - \xi\cos[\theta_s] - \theta_{s_o}\right\} \tag{66}$$

where for simplicity the following definition has been used:

$$\xi = \frac{\Omega R}{c}\sin\ \beta\ = M_T \sin\ \beta \tag{67}$$

Combining Eq. (42) with the general expression for the coefficients in Eq. (63) gives

$$A_n(r,\beta) = \frac{F\sin\gamma\sin\beta}{4\pi r_o c}\frac{1}{2}\pi e^{jn(\Omega r_o/c - \theta_{so})}\frac{\partial}{\partial t}\int_{-\pi}^{\pi}\sin[\theta_s]e^{-jn([\theta_s] - \xi\cos[\theta_s])}d[\theta_s] \tag{68}$$

In order to evaluate this Fourier integral it is most advantageous to use the following identity uniquely appropriate to circular sources, as introduced by Gutin.

$$e^{jn\,\xi\cos\theta_s} = \sum_{m=-\infty}^{\infty}(-j)^m e^{jm\theta_s}\ J_m(-n\xi) \tag{69}$$

Using (69) in (68) and interchanging the order of summation and integration allows the Fourier integral to be written as:

$$\frac{1}{2\pi}\int_{-\pi}^{\pi}\frac{e^{j(\theta_s - n\theta_s + m\theta_s)} - e^{-j(\theta_s + n\theta_s - m\theta_s)}}{2\ j}\ d\theta_s \tag{70}$$

This integral has a value of 1/2 only when $m = n \pm 1$, otherwise it is zero. Therefore in the evaluation of A_n, there appear two Bessel functions, which can be combined to give a single Bessel function of order n. The resulting far field acoustic pressure for one blade becomes;

$$p_a(r,\beta,t) = \frac{F\sin\gamma}{4\pi r_o R}\sum_{n=-\infty}^{\infty} n(j)^{n+1}e^{jn(\Omega(t - r_o/c) + \theta_{so})}J_n(n\xi) \tag{71}$$

If now the turbomachine is composed of B equally spaced, and equally loaded blades, the acoustic pressure is the sum over the individual θ_{so} positions. Since this sum is B for $n = lB$, and zero otherwise, the result is;

$$p_{aB}(r,\beta,t) = \frac{BF\sin\gamma}{4\pi r_o R}\sum_{l=-\infty}^{\infty} Bl(j)^{Bl+1}J_{Bl}(Bl\xi)e^{jBl\Omega(t-r_o/c)} \tag{72}$$

which is the classic Gutin solution to Eq. (42) for low M_T.

Some illustrative features of the acoustics of a single rotor in a free acoustic field can be obtained by examining Eq. (72). First of all, the leading term is the total force on the rotor blades, radiating in such a manner as to have the acoustic pressure decrease inversely with r_o . Secondly, the amplitudes of the steady term, $l = 0$, the fundamental, and the higher frequency terms are all indexed to the Bl product, with a spatial interference pattern given by the Bessel function of order Bl .

To interpret this result it is useful to know how Bessel functions behave versus their argument, as shown in Fig. 12 for J_o, J_1 and J_5 . The following asymptotic relationships are useful:

$$J_o(\xi) \approx 1.0 \quad \text{for}\, \xi = M_T\sin\beta << 1 \tag{73a}$$

$$| J_{Bl}(Bl\xi) | \approx \frac{(Bl\xi/2)^{Bl}}{Bl} \quad \text{for}\, Bl\xi < 1 \tag{73b}$$

$$| J_{Bl}(Bl\xi) | \approx \left(\frac{2}{\pi\xi Bl}\right)^{1/2} \quad \text{for}\, \xi > 1 \tag{73c}$$

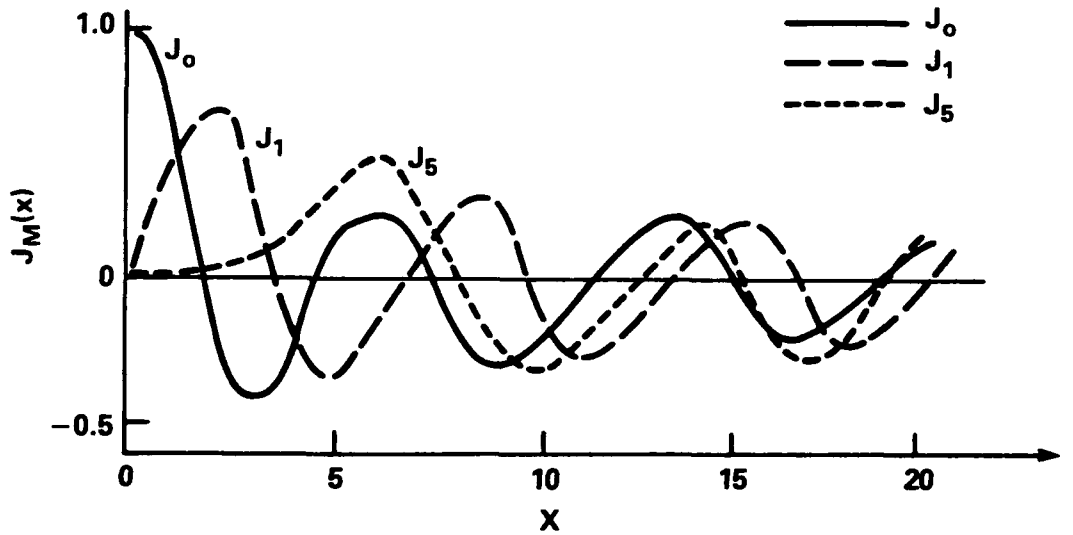

Fig. 12. Representative Bessel functions vs. argument.

Now, when l = o, the result is always zero since this index value multiplies each harmonic. As the harmonic index increases, with ξ still small, the amplitudes fall rapidly with increasing l. In all cases the acoustic pressure on the axis, $\beta = o$ will be zero. Since the Bessel functions oscillate about zero as the argument increases, the acoustic pressure exhibits a symmetric lobed pattern with increasing angle β. In general, as the harmonic number increases, the amplitudes of the pressure pattern will decrease quickly. The implication of the basic Gutin solution is that larger blade numbers should reduce the tonal acoustic pressure for the low tip Mach numbers of interest.

Stator In the Wake of a Rotor

The second arrangement to examine is that for a stator vane row situated downstream of a rotor. A convenient technique for this geometry was reported by Duncan and Dawson, who were concerned primarily with the total acoustic power radiated from unequally spaced blades, instead of a detailed description of the radiated acoustic pattern. Duncan and Dawson assumed an unsteady force, i.e., dipole, radiation from each stator, and that the force on any stator blade, q, was attributable to the wake from rotor blade, b. Figure 13 shows how the motion of each blade produces a variation in force on each stator as:

$$F_q(\theta_B)_{b=1} = \sum_{l=-\infty}^{\infty} B_l e^{jl(\theta_B - \theta_q)} \tag{74}$$

Here the Fourier coefficient is

$$B_l = F(l) = \int_{-\infty}^{\infty} f_q(\theta_B) e^{-jl\theta_B}\, d\theta_B \tag{75}$$

Where $f_q(\theta_B)$ is the single event blade-vane interaction centered at $\theta = o$ and $t = o$, and the event is repeated for every $\Delta\theta = 2\pi$. If now there are B equal and equally spaced blades, the summed force on any stator vane is;

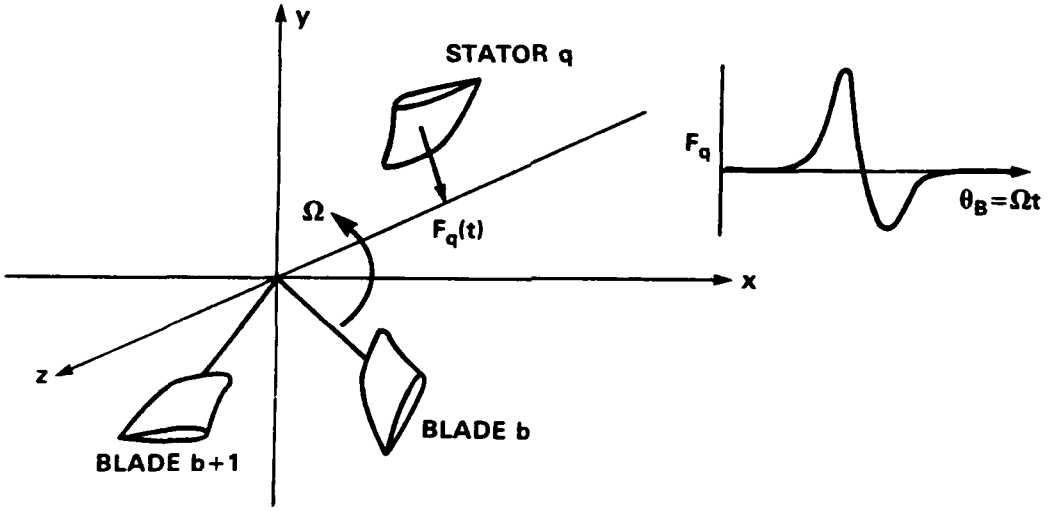

Fig. 13. Interaction force on stator vane from blade rotation.

$$F_{qT}(\theta_B) = \sum_{l=-\infty}^{\infty} B_l \sum_{b=o}^{B-1} e^{jl(\theta_B+\theta_b-\theta_q)} \tag{76}$$

Since $\theta_b = 2\pi b/B$ and $\theta_b = \Omega\ t$, the sum is non-zero only for l = nB such that;

$$F_{qT}(t) = B \sum_{n=-\infty}^{\infty} B_{nB} e^{jnB(\Omega t-\theta_q)} \tag{77}$$

gives the force, and therefore the dipole strength on each stator vane. From (42) it is known that this force is radiated with the acoustic delay time:

$$\tau_q = r_o/c - \frac{R\sin\beta}{c}\cos(\psi-\theta_q) \tag{78}$$

Therefore the far-field acoustic pressure is:

$$p_a(r,t) = \frac{jB\Omega}{4\pi r_o c} \sum_{n=-\infty}^{\infty} (\vec{n}_o \cdot \vec{n}_q) nBB_{nB} e^{jnB(\Omega(t-r_o/c)+\xi\cos(\psi-\theta_q))} \tag{79}$$

where ξ is defined in Eq. (67). The direction vector product is;

$$\vec{n}_o \cdot \vec{n}_q = \cos\gamma\cos\beta + \sin\gamma\sin\beta\sin(\psi-\theta_q) \tag{80}$$

which again represents axial and tangential force components. Introducing the Gutin Bessel function identity from Eq. (69) and summing over all V equal vanes gives;

$$p_a(r,t) = \frac{jB\Omega}{4\pi r_o c} \sum_{n=-\infty}^{\infty} nBB_{nB} e^{jnB\Omega((t-r_o/c)} \sum_{m=-\infty}^{\infty} (-j)^m J_m(nB\xi) \sum_{q=o}^{V-1} \vec{n}_o \cdot \vec{n}_q e^{j(m(\psi-\theta_q-nB\theta_q)} \tag{81}$$

Comparing the overall features of (81) and (72), it can be seen again that the acoustic pressure varies inversely with r_o , and that the Bessel function behavior is symmetric about the plane of rotation.

Inspecting (81) in more detail, it can be seen that the sum over all vanes for the axial term, $\beta = o$, of (80) will be zero, except for;

$$m + n\ B = \pm\ kV \tag{82}$$

In this case, when the blade and vane numbers are equal, or they have some common multiple, the index m = o occurs, and the J_o term can appear. This corresponds to a condition where *all the blade wakes and vanes overlap axially at the same time such that there is unified dipole radiation in the axial direction.* Compared with the rotor alone, this radiation can be quite strong, even at low Mach numbers, because of (73a). However it has been known for some time that this tonal source can be eliminated by making V > 2B such that these J_o terms do not develop. Of course, the strength of each harmonic will vary with sharpness of the wake pulse coefficient, B_{nB} , which is in turn related to a Sears function response.

Turning to the torque term, Eq. (80) the indexed position of each source relative to an observer in the x–z plane, i.e., when $\psi = 0$ introduces conditions such that the sum over all vanes is non-zero when:

$$m = n\ B + kV + 1 \tag{83}$$

Again there is the possibility for m = o, and J_o to appear when the blade and vane number combinations are separated by an integer of one. The implication here is that the radiation in the radial direction at frequency $nB\Omega$ behaves as a rotating dipole. Again, the harmonic strength depends on $B_{n\,B}$, and the Bessel function order can be kept large when $V > 2B$.

Rotor in a Non-Uniform Inflow

The last free-field radiation case to examine is that for a rotor operating in a steady, but non-uniform, inflow as shown in Fig. 14. The inflow distortion can be described by circumferential harmonics of the form of (84) if it is deterministic:

$$\delta v_{IN} = v_w \cos w[\theta_s] \tag{84}$$

When this distribution modulates the steady blade force used in the Fourier integral of (68), the $\sin\theta_s$ term from the steady force acquires a perturbation component.

$$\delta F\left(\frac{1}{2}\sin\ (w+1)\theta_s - \frac{1}{2}\ \sin(w-1)\theta_s\right) \tag{85}$$

Using this in Eq. (70), it can be seen that the only Bessel function orders having non-zero coefficients are:

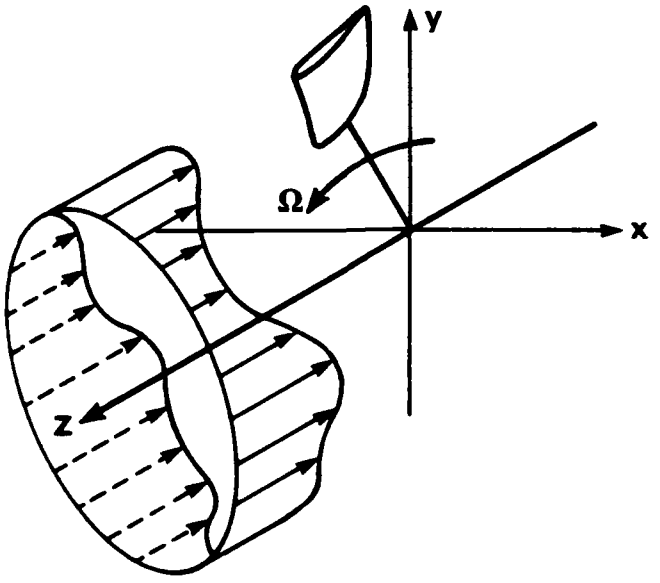

Fig. 14. Rotor blade operating in a non-uniform deterministic inflow.

$$m = n + (w + 1) \qquad (86)$$

$$m = n + (w - 1)$$

By combining the resulting Bessel functions, and summing the acoustic signals from B equally spaced blades, the far-field pressure is;

$$p_a(r,t) = \frac{\delta F B \sin\gamma}{4\pi r_o R} \sum_{l=-\infty}^{\infty} \frac{Bl}{2} \left(J_{Bl+w}(lB\xi) - J_{Bl-w}(lB\xi) \right) (j)^{Bl+1} e^{iBl\Omega(t-r_o/c)} \qquad (87)$$

From (87) it can be seen that if the inflow disturbance number is some multiple of B, then J_o terms appear and strong on-axis dipole radiation occurs, even at low Mach number. However, even if B and w have no common multiples, but are such that low order Bessel terms appear, i.e., J_1, or J_2, then some significant acoustic radiation can still occur at blade passing frequencies, being strongest in the radial direction.

CYLINDRICAL DUCT

When the turbomachine rotor is located within a duct system it is necessary to account for the boundaries in computing solutions to Eq. (42). For internal flow the simplest geometry is the rotor in an infinitely long cylindrical duct with rigid walls. This geometry is appropriate for axial flow machines, but for centrifugal devices a toroidal volute is often present between inlet and exit ducting. That geometry produces its own unique acoustic cavity behavior, which must be examined separately using, for example, the finite element approach of Everstine. In the present study the focus will be limited to axial flow machines in a cylindrical duct.

Tyler and Sofrin Rotor-Stator Tones

The classic solution to the acoustic radiation from an axial flow rotor, or rotor-stator combination, in a duct is that of Tyler and Sofrin. Their approach considers first the general question of acoustic propagation of unsteady pressure patterns in a cylindrical duct, rather than specific blade dipoles. Thus it is found that only certain circumferential mode shapes, associated with specific radial Bessel function patterns, will propagate over significant axial distances. In particular, only those compatible radial and circumferential pressure distributions that appear to rotate at greater than sonic speed are found to propagate axially. Thus a rotor-locked pressure field, i.e., steady in the rotating frame, will propagate only if the rotor speed is supersonic. On the other hand, the stator-locked pressure field, which behaves as a standing wave system excited at blade passing frequency, can be thought of as two oppositely rotating pressure fields since;

$$\cos(B\Omega t)\cos\frac{2\pi R\theta}{\lambda_w} = \frac{1}{2}\left[\cos\left(B\Omega t + \frac{2\pi R\theta}{\lambda_w}\right) + \cos\left(B\Omega t - \frac{2\pi R\theta}{\lambda_w}\right)\right] \qquad (88a)$$

Rewriting the second term gives, for example;

$$\cos\left[\frac{2\pi}{\lambda_w}\left(\frac{B\Omega\lambda_w}{2\pi}t - R\theta\right)\right] = \cos\left(\frac{2\pi}{\lambda_w}(V_w t - R\theta)\right) \qquad (88b)$$

so that the apparent circumferential Mach number for a pressure wave length λ_W is:

$$M_W = \frac{V_w}{c} = \frac{B\Omega}{c}\frac{\lambda_w}{2\pi} = \frac{\lambda_w}{\lambda_{a_B}} \tag{88c}$$

Therefore when the circumferential wavelength of any Fourier pressure component exceeds the acoustic wavelength for a frequency corresponding to the repeating blade exitation rate, then the wave speed will appear to be supersonic. The result is that smaller spatial wavelength disturbances will not propagate.

With the above criteria in mind, Tyler and Sofrin assume that the rotor/stator system of Fig. 15 will create the following annulus pressure modes for the interaction of the blade row with a single vane located at the angular origin;

$$p_q(\theta, t) = \sum_{n=-\infty}^{\infty} A_n(\theta) e^{j2\pi nt/T_o} \tag{89}$$

where $T_o = 2\pi/B\Omega$. Further, it is assumed that each Fourier coefficient in Eq. (89) can be described by a second combination of circumferential harmonics;

$$A_n(\theta) = \sum_{m=-\infty}^{\infty} B_{n(m)} e^{jm\theta} \tag{90}$$

If this arbitrary pressure pattern is now summed for multiple identical stators with angular separation of $\Delta\theta = 2\pi/V$, and time delay $\tau = \Delta\theta/\Omega$ from the start of the sequential events, the annulus pressure is:

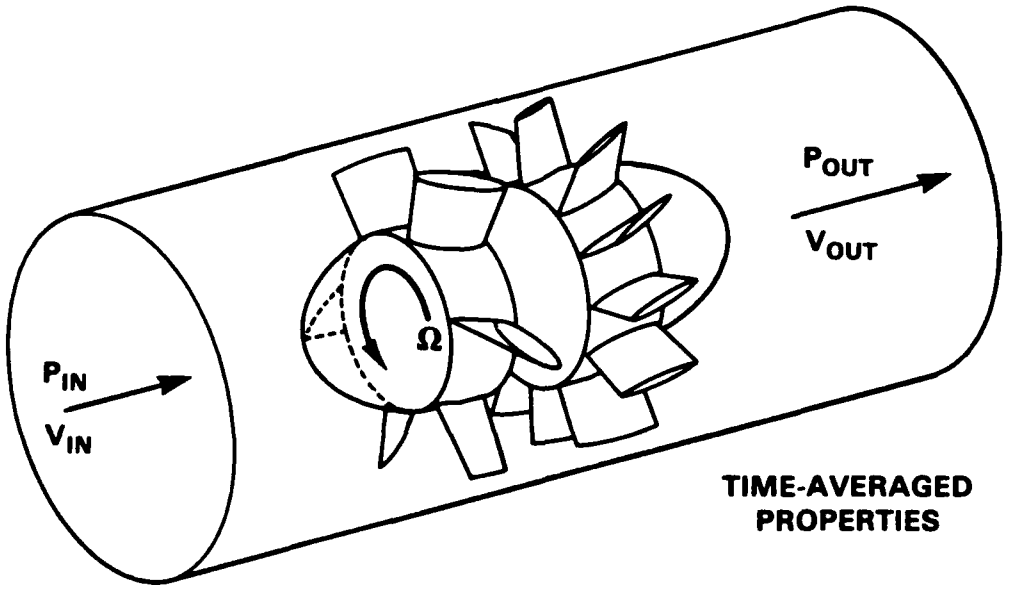

Fig. 15. Multibladed rotor acting on a stator vane in an infinite duct.

$$p_t(\theta,t) = \sum_{n=-\infty}^{\infty} \sum_{m=-\infty}^{\infty} B_{n_m} \sum_{q=o}^{V-1} e^{j(m(\theta - q\Delta\theta) + nB\Omega(t + q\Delta\theta/\Omega))} \tag{91}$$

Combining terms into appropriate summation groups gives

$$p_t(\theta,t) = \sum_{n=-\infty}^{\infty} \sum_{m=-\infty}^{\infty} B_{n_{(m)}} e^{jm(\theta + \frac{nB\Omega}{m}t)} \sum_{q=o}^{V-1} e^{-j(m-nB)2\pi q/V} \tag{92}$$

From Eq. (92) it is clear that the sum over all the vanes of the last term will be zero unless;

$$m = nB + k\ V \tag{93}$$

for which it has the value V. Additionally, from the mode summation exponent it can be seen that the apparent speed of rotation of the mth mode shape is;

$$V_m = \frac{nB}{m}\ \Omega R \tag{94}$$

where, from the initial acoustic analysis, that mode will propagate if $V_m > c$.

Even though the Tyler & Sofrin results are very simple, quite a bit can be learned from their examination. For example, Eq. (94) indicates that all modes satisfying the m = o condition will propagate, effectively as plane waves, since λw is infinite. This is similar to the appearance of J_o radiation by Eq. (82) for the free-field problem. This mode is associated with thrust and torque fluctuations on the stator from all vanes acting together. Inspection of Eq. (93) shows that m = o when B and V are equal, or have some common multiple. In case neither of the above criteria is met, then the first value of blade harmonic n that gives m = o will be V, and the BV harmonic will radiate, although the amplitude B_{nB}, may be small. Continuing, if there is one blade that differs from the others, then $B = 1$ is appropriate and m = o occurs for $n = V$ such that *vane frequency* propagates. On the other hand if there is one odd vane, then $V = 1$ and $m = o$ occurs for $k = B$ and $n = 1$ such that *blade frequency* propagates. For the rotor-only case, $V = o$ and Eq. (94) indicates that with $m = nB$, the rotor tip speed must be supersonic for any radiation to propagate in the cylindrical duct. Finally, even if m = 1, 2, 3, ... propagation can still occur if V_m from Eq. (94) is greater than c. In such cases the wave fronts are angled to the duct axis, therefore giving rise to the term "spinning modes."

As a general conclusion, Tyler and Sofrin predict that, for a subsonic rotor-stator combination in a duct, tonal acoustic radiation can be prevented to a large degree when V > 2B. This rule is similar to the free-field result of Eq. (82), which shows that the V > 2B criteria will prevent J_o terms, and their strong radiation. It also provides a constraint in the free-field that only higher order Bessel terms, with their lower amplitudes, will appear for subsonic turbomachines. According to Cumpsty this result has been known and used for many years in the aircraft literature.

Goldstein's Classic Analysis

The approach of Tyler and Sofrin is one way to represent the effect of multiple dipoles acting as a phased planar array in a rigid cylindrical duct. The success of their analysis suggests that the exact nature of the pressure field, either near or far, is not as

important as is the spatial pattern and the time delays. In fact, Tyler and Sofrin are vague about just where the pressure pattern is defined to start, do not directly require the Gutin identity of Eq. (69), and therefore do not produce Bessel functions as such, with physically derived dipole force coefficients. Of course the Bessel function for the duct problem will be different than for the free field, the pressure will not vary inversely with distance, and the distinction between axial and radial directivity will not exist.

These uncertainties and similarities have been resolved by Goldstein who develops exact analytic solutions for the rotor-stator problem in finite and infinite length ducts. Using traditional separation of variables techniques, Goldstein starts from local blade forces in terms of torque and thrust, and expresses the radial pressure patterns in terms of Bessel functions. Applying the boundary condition of zero radial velocity at the rigid duct wall requires that the pressure gradient also be zero, and therefore that the *first derivative* of each Bessel function be zero at the wall. Since Bessel functions oscillate radially, there is an infinite series of zeros for each order. These radial root numbers enter into the axial propagation function such that there will be rapid decay of the mode when:

$$(1-M^2)\ K_{m,s} > k_o^2 = \left(\frac{\omega}{c}\right)^2 = \left(\frac{nB\Omega}{c}\right)^2 \tag{95}$$

Here, $K_{m,s}$ is the s order zero of the first derivative of J_m. Goldstein points out that $K_{m,s}$ tends to infinity with m or s such that only the initial roots need be examined. Since the first zero turns out to always be larger than m/R, propagation will not occur when

$$\left(1-M^2\right)\left(\frac{m}{R}\right)^2 > \left(\frac{nB\Omega}{c}\right)^2 \tag{96}$$

Examining the Bessel function orders m, that describe the force distribution, Goldstein shows that for a deterministic inflow distortion of circumferential order w, the following are permissible;

$$m = nB + w \tag{97a}$$

and for a rotor-stator system of V vanes the Bessel function orders are again:

$$m = nB + kV \tag{97b}$$

In all cases there will be propagation along the duct axis when:

$$\left(\frac{nB}{m}M_T\right)^2 > 1 - M^2 \tag{98}$$

Therefore for the rotor by itself in a uniform flow, i.e., V = o, there will be propagation in the duct when

$$M^2 + M_T^2 = M_{rel}^2 > 1 \tag{99}$$

For wake or vane generated force oscillations there will always be plane wave propagation and thrust oscillations when the J_o terms occur. When higher order Bessel function shapes satisfy Eq. (98) the propagation will occur in the form of "spinning modes" as described first by Tyler and Sofrin and illustrated in Fig. 16.

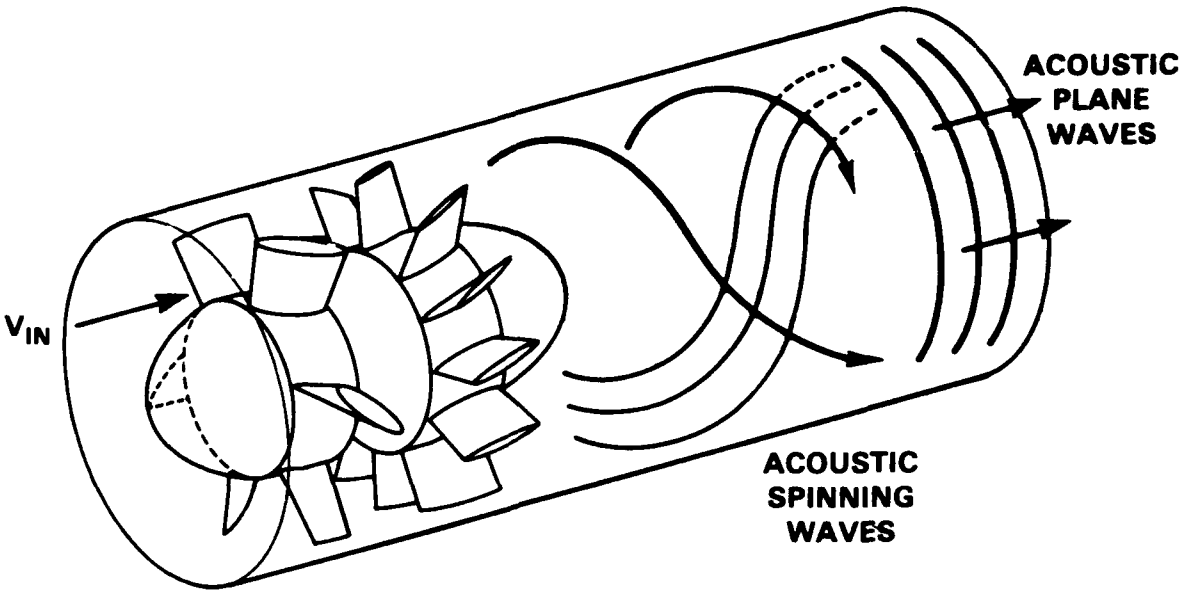

Fig. 16. Propagation of plane and spinning acoustic waves from rotor-excited sources in a duct.

While Goldstein reaches much the same conclusions as Tyler and Sofrin, his analysis is more definitive in that the forces responsible for the acoustic waves are identified. Thus the coefficients of each Bessel function are exactly the linear coefficients of the blade response to a periodic change in upstream velocity. Hence all coefficients depend upon a Sears function solution for the blade or vane row, such that the amplitudes will decrease rapidly with reduced frequency greater than one.

In summary, the analysis of Goldstein for turbomachine acoustics in a duct agrees with Tyler and Sofrin, but provides the necessary details on the dipole nature of the acoustic source. For the rotor-stator combination, the conclusion remains that tonal radiation should not occur for $V > 2B$. Machines that exhibit tones, even though this criterion has been met, are believed to be influenced by steady inflow distortions or by large scale turbulence. As alluded to earlier, the major tonal difference between a rotor-stator combination and a stator-rotor combination is that the harmonic thrust coefficients are indexed in nB for the former and kV for the latter, but in all cases the radiation must occur with period determined by the moving member. Finally, for all interference analyses in systems with circular symmetry the presence of Bessel functions describes the interaction of discrete and perfect geometries. In real physical systems many imperfect conditions occur which tend to blur these results. When the turbomachines have been designed to eliminate first and second order acoustic signals, then other types of propagation analysis may be more appropriate than the perfectly harmonic ones described above.

VORTEX CONCEPTS IN REAL TURBOMACHINES

VORTICES AND PERFORMANCE

The previous analysis showed how the flow structure of unsteady vortex loops is associated with the work output and the tonal acoustics of turbomachines for some simple cases. While this provided an insight into the large scale flow mechanisms involved, there remains the question of how these concepts can help to define the details of real machines where the fluid has rotationality, viscosity and turbulence. From a larger perspective, this complete problem is usually investigated by quantitative flow visualization or by computational fluid dynamics, CFD. With the advent of modern computers, the latter technique allows the simultaneous solution of the full mass, momentum and energy conservation equations in detail by specifying only the behavior of the fixed and moving boundaries. The continuing work of Lakshminarayana and Thompson, and Rai, and co-workers are representative of CFD developments directly applicable to the turbomachines of interest herein. Although these diagnostic techniques, experimental or computational, can give more realistic results than a potential flow analysis, some of the phenomena unique to turbomachine performance and acoustics can still be appreciated most readily in terms of basic vortex/dipole principles.

Turbulence

One of the major differences between potential flow theory and real fluids is turbulence. Interestingly, turbulence by itself does not affect significantly the time-average work output of most turbomachines. It seems that the dynamic behavior of the turbulent-flow flow field is represented properly by a Sear's function type of potential flow force and work response. Therefore this primarily linear three-dimensional behavior is space and time averaged by the blades to give the same overall energy transfer as with steady flow. For the acoustic output, the answer is different. As demonstrated earlier in Eq. (42), the far-field acoustic wave depends on the time derivative of flow field parameters. Thus because the nature of turbulence is unsteady flow, the acoustic output from a turbulent flow is fundamentally different from that of a steady flow. To illustrate, for a blade row, stationary or moving, the time variations associated with inflow turbulence produce lift fluctuations that radiate as uncorrelated impulses. These have only a limited similarity to the deterministic flows analyzed previously.

Stationary Blades

A second significant difference from potential flow is that rotationality or distributed vorticity, is often present in the fluid, especially when viscosity and boundary layers are important. For example, if the inflow to a blade row contains vorticity normal to the mean flow, the turning action of a blade row can, by conservation of angular momentum, convert this into secondary vortex motion with axis in the flow direction, as shown in Fig. 17. This is of interest since the inflow to a cascade usually contains boundary layers on the inner and outer walls, with oppositely directed vorticity. Then two oppositely rotating axial vortices will form at the inner and outer ends of the blade span. These vortices will then be convected downstream with the mean flow. In addition, the inflow boundary layer velocity profile approaching a right-angle blade-boundary wall corner junction will cause the formation of a horseshoe vortex as the flow splits to pass on either side of the blade. Further, if the bound vortex distribution is non-uniform along the blade span, vorticity

will be shed from the trailing edges and a sheared flow will exist downstream. Finally, if the rate of pressure rise or the turning through a blade row is too great in the flow direction, the newly-formed blade boundary layer can experience reverse flow and large separated-flow vortex structures can be generated in an unsteady fashion. All of the above can occur for stationary and moving blade rows, as shown in Fig. 18. The result is that the downstream flows of real fluids can have considerable new vorticity, which may be inherently unstable, leading to losses and sources of sound. Moreover, for separated flows where there may be large dynamic pressure forces appearing on the blades, strong acoustic dipole radiation can occur from each impulsive event.

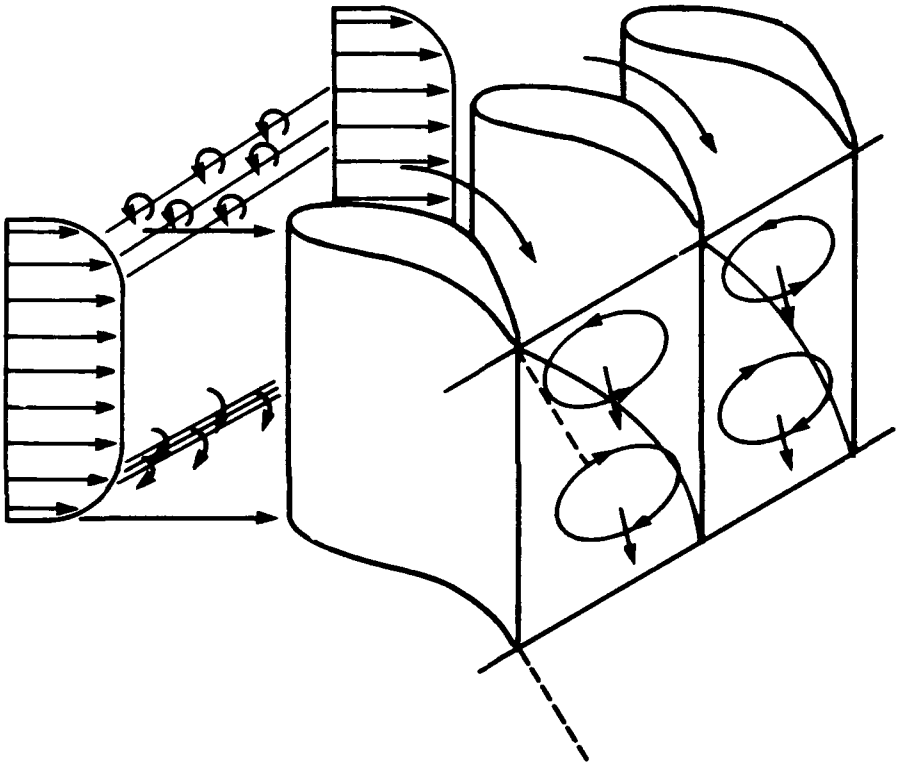

Fig. 17. Conversion of inlet vorticity by a turning vane row.

Rotating Blades

When blades rotate, additional secondary flows appear with real fluids because of the unique action of the moving boundary with viscous surface layers. First, the boundary layer on a rotating blade is affected more by the centrifugal force than the through-flow. Depending on the machine geometry and surface pressures, this force field tends to set in motion a large channel vortex system with axis in the mean flow direction. Secondly, for blades with significant tip clearance, some of the bound vortex system can be shed around the tip, resulting in a region of high shear at the wall. (For the ideal internal flow machine, where the blade is loaded uniformly, this vortex is shed mathematically into the outer boundary and does not cause complex flows.) Also important for the moving blade case is the fact that the boundary layer leaves the trailing edge in a manner different than

for a stationary blade, a fact that is often overlooked. This is because when viewed in the absolute frame, as in Fig. 19, the boundary layer fluid is attached to a moving surface and represents a high energy flow moving at some angle to the bulk fluid. Clearly the details of the trailing edge dynamics in this case are different than for flow over a stationary blade. Finally, it has been observed that for certain flow conditions turbomachines develop large vortex structures outside of the blade row that rotate in the same direction as the shaft, but at some lower speed. These vortex systems are called "rotating stall" and can produce very strong dynamic effects at the inlet or the exit.

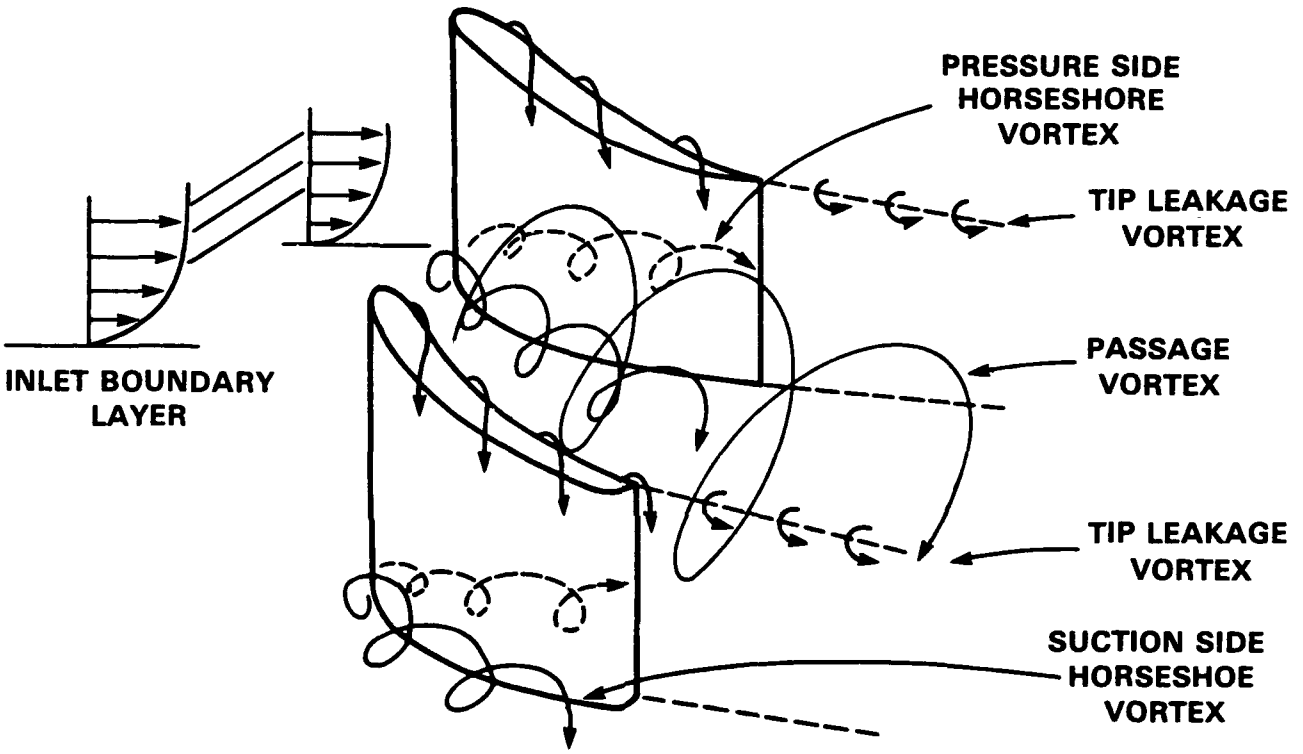

Fig. 18. Combination of blade row vortex systems.

All of the above effects represent a transfer of fluid energy into new vortex or shear layer flows from which that energy cannot be recovered in any practical manner. Moreover, these complex flows tend to be naturally unstable and to be dispersed by turbulence, eventually being dissipated by viscosity. The literature on turbomachinery contains extensive studies, experimental and theoretical, on these "secondary" flows since they are so important to machine efficiency. As observed by Atassi in a recent review of the Sear's function properties,

> "The circulation around the airfoil changes in response to every unsteadiness in the flow. For every change in circulation, a vortex must be shed at the trailing edge of the airfoil and is carried away by the mean flow. Therefore vortices shed in the wake represent a recorded history of the airfoil non-uniform motion."

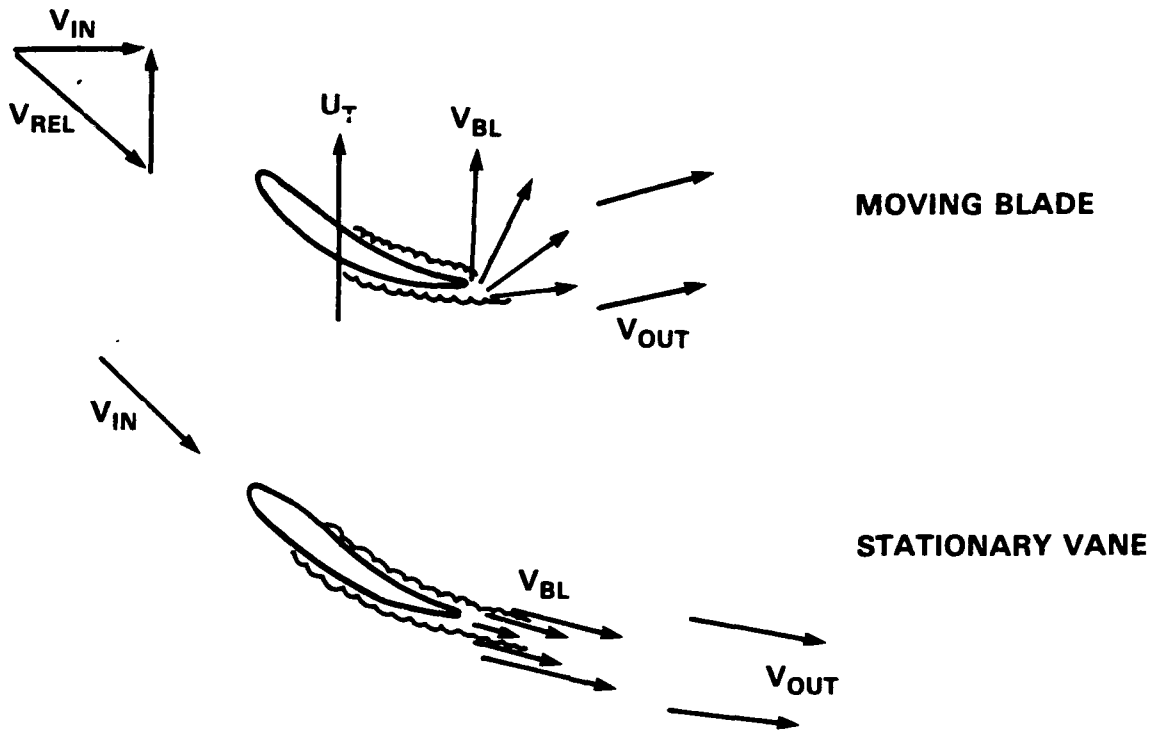

Fig. 19. Trailing edge absolute velocities for stationary and moving airfoils.

Although stated for unsteady flow, this observation applies to all the shed vortex systems, since each produces its own wake signature. It is just this effect that the Lighthill vorticity moment integral, Eq. (28), is intended to capture for a single blade surface. For a complete turbomachine, which on the average introduces torque and thrust, the result in the wake is a history of impulses from each blade and vane, along with any duct boundary conditions, to yield a total flow field with changed energy and momentum.

VORTICES AND ACOUSTICS

From the acoustic standpoint, the real turbomachine generates primarily the work–related vortex system predicted from potential flow theory. But in addition, the set of secondary vortices discussed above appears in a complex manner that is difficult to categorize in terms of total fluid acoustic behavior. One approach to assessing the overall unsteady acoustics is to assume that each blade can be described analytically by a time and space distribution of externally applied volume and force sources. Thus the mass and momentum conservation equations become:

$$\frac{\partial p}{\partial t} + \vec{\nabla} \cdot \rho \vec{V} = \dot{m}\,(x,t) \tag{100}$$

$$\frac{\partial \rho \vec{V}}{\partial t} + (\vec{\nabla} \cdot \rho \vec{V})\,\vec{V} = \vec{\nabla} p + \mu \nabla^2 \vec{V} + \vec{f}\,(\vec{x},t) \tag{101}$$

For flows where the density changes and Mach numbers are small, the time derivative of Eq. (100) and the divergence of Eq. (101) can be combined to give;

$$\nabla^2 p - \frac{1}{c^2}\frac{\partial^2 p}{\partial t^2} = -\varrho_o \vec{\nabla} \cdot \left(\vec{\nabla}(V^2/2) + \vec{\xi} \times \vec{V} - \frac{\mu}{\varrho_o}\nabla^2 \vec{V} \right) - \frac{\partial \dot{m}}{\partial t} + \vec{\nabla} \cdot \vec{f} \quad (102)$$

In this inhomogeneous form of the wave equation, the terms on the right represent distributed acoustic sources. If the source activity is limited to a small region near the origin, and the intervening fluid is uniform and stationary, then a Helmholtz integration, with the delay times retained, over the active fluid region, and assuming acoustically compact surfaces, gives

$$p_a(r,t) = \frac{1}{4\pi r_o}\left\{ \int\int\int \varrho_o [\vec{\nabla}_y \cdot (\vec{\nabla}(V^2/2) + \vec{\xi} \times V - v/\varrho_o \nabla^2 \vec{V})]_{t-r/c} d\forall + \right. \quad (103)$$

$$\left. \int\int\int [\vec{\nabla}_y \cdot \vec{f}]_{t-r/c} d\forall - \int\int\int \left[\frac{\partial \dot{m}}{\partial t} \right]_{t-r/c} d\forall \right.$$

Equation (103) is a general result for far-field radiation from a small source, but to appreciate its meaning it is useful to consider some simple cases.

Rigid Sphere

First, let the source be the *rigid sphere oscillating in an inviscid fluid.* The first volume integral is to be taken over all the fluid outside the sphere using a singly-connected region that contains no singularities. Doing this for the case of low Mach number results in the integral being negligible for an irrotational and inviscid flow. The second integral involving the divergence of the force vector can be converted to a propagating time derivative by recognizing that in the far-field;

$$\vec{\nabla}_y \cdot = -\vec{\nabla}_x \cdot = \frac{\vec{n}_o}{c} \cdot \frac{\partial}{\partial t} \quad (104)$$

Taking the second integral over the surface of the sphere gives the net force vector with the correct time delay:

$$\int\int\int [\vec{\nabla}_y \cdot \vec{f}]_{t-r/c} \, d\forall = \frac{1}{c}\frac{\partial}{\partial t}\vec{n}_o \cdot \int\int [p_o \vec{n}_s]_{t-r_o/c} \, ds = \frac{1}{c}\frac{\partial}{\partial t} [\vec{n}_o \cdot \vec{F}_A]_{t-r_o/c} \quad (105)$$

Examination of the last integral of Eq. (103) shows that it represents the mass introduction to the region, which for a constant volume sphere will be zero. However, as discussed earlier the linear motion of the sphere is simulated by mass introduced at the front and removed at an equal rate at the back. The acoustic time delay operation on this behavior results in the time derivative of the first moment of the surface integral of mass addition in the direction of the observer.

$$\int\int\int \left[\frac{d\dot{m}}{dt} \right]_{t-r/c} d\forall = \frac{\vec{n}_o}{c} \cdot \frac{\partial}{\partial t} \varrho_o \int\int \left[\frac{\partial u_n}{\partial t} \vec{s} \right]_{t-r_o/c} ds = \frac{\vec{n}_o}{c} \cdot \frac{\partial}{\partial t} \left[\varrho_o \Delta \frac{d\vec{u}}{dt} \right]_{t-r_o/c} \quad (106)$$

Therefore the total far-field acoustic pressure for a moving solid sphere is;

$$p_a(\vec{r},t) = \frac{\vec{n}_o \cdot}{4\pi r_o c}\frac{\partial}{\partial t}\left[\vec{F}_A + \varrho_o \Delta \frac{d\vec{U}}{dt}\right]_{t-r/c} = \frac{\vec{n}_o \cdot}{4\pi r_o c}\frac{\partial}{\partial t}[\vec{F}_s]_{t-r_o/c} \qquad (107)$$

This can be recognized as the combined added and displaced mass terms in the Lighthill equation for the force on a moving rigid body. (Eqs. (26a) and (26b) or Eq. (48)). Interestingly, these two force vectors need not be in the same direction, since the added mass term responds to the relative velocity.

Moving Airfoil

Taking next the case of a *moving airfoil of zero thickness*, the volume-related terms are neglected, but the integration of Eq. (103) must now account for the divergence of the work force vector due to the relative flow over the airfoil. This can be computed as above so that:

$$\int\int\int [\vec{\nabla}_y \cdot \vec{f}_w]_{t-r/c} d\vec{V} = \frac{\vec{n}_o \cdot}{c}\frac{\partial}{\partial t}\int\int [p_w \vec{n}_s]_{t-r_o/c}\, ds = \frac{\vec{n}_o}{c} \cdot \frac{\partial}{\partial t}[\vec{F}_w]_{t-r_o/c} \qquad (108)$$

For a moving airfoil, the vorticity in the first integral of Eq. (103) is somewhat more difficult to interpret since the work force can produce vorticity in the fluid. When there is vorticity distributed in the fluid, it may be recalled that;

$$\int\int \zeta dA = \Gamma n_v \qquad (27b)$$

where the surface integral is taken such that the vorticity is normal to the surface, and the singularity strength Γ represents all the vorticity in that area. If now the local shed vorticity vector is aligned with the local velocity, as for a fixed blade, or if there is no shed vorticity in the fluid, as for a blade with spanwise uniform circulation, the first volume integral is again negligible. Alternately, if the blade is of finite span, and moving, the shed vorticity will include both positively and negatively rotating parts. These will be at some angle to the velocity and must be present to account for the span-wise enthalpy distribution. As a consequence, over the volume of integration both positive and negative span-wise force components will appear in the wake. Once introduced into an ideal fluid, this pattern of opposing forces will not change, except for convection. Therefore it will not produce a significant first-order time derivative when Eq. (104) is applied to the volume integral of the vorticity-velocity cross product. Hence for an airfoil of negligible volume, evaluation of Eq. (103) yields only:

$$p_a(\vec{r},t) = \frac{\vec{n}_o \cdot}{4\pi r_o c}\frac{\partial}{\partial t}[\vec{F}_w]_{t-r/c} = \frac{\vec{n}_o \cdot}{4\pi r_o c}\frac{\partial}{\partial t}\left(\frac{\varrho_o}{2}\frac{\partial}{\partial t}\int\int\int [\vec{x} \times \vec{\zeta}]_{t-r/c}\, d\vec{V}\right) \qquad (109)$$

where the Lighthill vorticity moment integral is to be taken over all the volume, and includes the internal bound and the external shed vorticities.

Combining the above effects for a basic ideal turbomachine, the total dipole acoustic sources associated with one rigid blade are found to be due solely to forces applied to the fluid from without.

$$\vec{F}_{(t)} = \int\int p\vec{n}_s ds + \varrho_o \Delta \frac{d\vec{U}}{dt} = \frac{\varrho_o}{2}\frac{\partial}{\partial t}\int\int\int (\vec{x} \times \vec{\zeta}) d\forall + \varrho_o \Delta \frac{d\vec{U}}{dt} \qquad (110)$$

These forces cause the expanding vortex loops necessary when there is work addition to the fluid and include the primary and secondary flows. They also represent the motion of the fluid mass displaced normal to the blade, along with the blade surface vortex loops necessary to produce the correct surface tangential velocity. In typical turbomachine designs the volume-related term will be small when compared with the work term.

Turbulent Sources

Clearly, in regions of the flow where there are no surfaces, $\dot{m} = f = o$, and the only acoustic sources will be the natural fluid instabilities, combined with turbulence. In this case only the first integral of Eq. (103) is needed to represent the dynamic forces involved for internally interacting fluid motions. The terms are the vector form of the well-known Lighthill stress tensor representation of the same phenomena, i.e.,

$$\varrho_o \vec{\nabla} \cdot \left(\vec{\nabla}(V^2/2) + \vec{\zeta} \times \vec{V} + \frac{\mu}{\varrho_o} \nabla^2 \vec{V} \right) = \frac{\partial^2 (\varrho_o U_i U_j + \tau_{ij})}{\partial y_i \partial y_j} = \frac{\partial^2 T_{ij}}{\partial y_i \partial y_j} \qquad (111)$$

Thus, away from surfaces the instabilities in real fluids produce an assembly of opposing motions that vary with time in their magnitude, location and direction. In these motions it is unclear how to distinguish between kinetic energy and vorticity transport terms, hence the utility of the stress tensor form that accounts for both. If the inflow to the machine is naturally turbulent then these local velocity fluctuations will cause fluctuating pressure distributions, and an altered pattern of wake vortices as described by Atassi. In addition, fluctuating flow across the solid body will cause added mass impulse pressures to appear. Figure 20 illustrates these acoustic sources for a blade row. It is possible that these unsteady sources can be clarified by CFD methods such as large eddy simulation or direct numerical simulation of turbulence.

In summary, many vortex systems occur for flows through turbomachinery, and many levels of analysis exist to understand and control these. The combined techniques of potential and real fluid analysis, as characterized by the many contributions of Howe seem to be an effective way to develop a building block approach to acoustic performance. Suffice it to say that the first acoustic goal should be to avoid the generation or propagation of tonal signals associated with shaft rotation. The second acoustic requirement should be to understand the sources of broadband noise and to develop innovative designs that suppress these sounds.

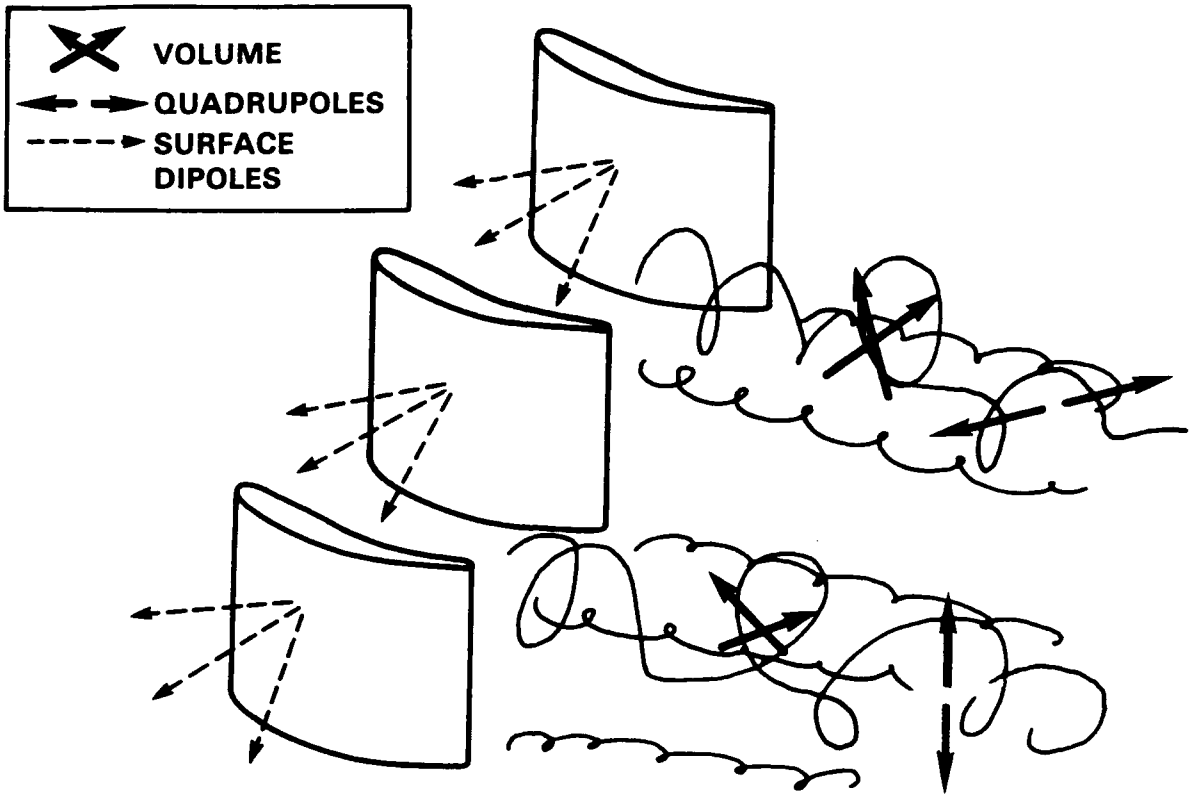

Fig. 20. Surface force dipoles and bulk flow quadrupoles.

CONCLUSIONS

The principles of unsteady potential flow theory provide a convenient and unified approach to understanding the work and acoustic properties of turbomachinery. The classic mathematics of Lamb, augmented by the contemporary work of Lighthill, and combined with specific applications by other investigators provides a reasonably complete analytical description of ideal turbomachines. From this it can be seen that all of the energy transfer functions of rotating machinery are related to moving and expanding three-dimensional closed loop vortex systems originating from the torque and thrust forces on each discrete blade. Although the internal details of the flow field differ between axial and centrifugal machines, the forces can be generalized by considering their origin on each blade, and the combination of their shed vortex loops to produce the total enthalpy change in the external flow.

In the mathematical models for these unsteady potential flows there exists a near–field solution that accounts for the work done, and a far-field solution representing the acoustic behavior. Because of the mathematical equivalence between vortex loops and combinations of dipoles, it is straight forward to show how the acoustics are derived from the work-related flow fields. The basic acoustic result for propagation into a three–dimensional field due to a dynamic force applied near the origin is the dipole pressure given by:

$$p_a(\vec{r},t) = \frac{\vec{n}_o \cdot}{4\pi r_o c}\frac{\partial}{\partial t}\,[\vec{F}(t)]_{t-r/c}$$

Fortunately, at geometrically remote points a single force can account for the work and volume displacement effects of a single blade moving through a fluid field. That force can be computed from a knowledge of the pressure distribution on the blade, or from an expression developed by Lighthill that uses kinematic flow variables from the entire fluid field;

$$\vec{F}_{(t)} = \int\int p\vec{n}_s ds = \frac{\varrho_o}{2}\frac{\partial}{\partial t}\int\int\int (\vec{x} \times \vec{\zeta}) d\forall + \varrho_o \Delta \frac{d\vec{U}}{dt}$$

Even though the initiating force may be well-defined, solutions for the far–field acoustics are complicated by the need to account properly for the delay time operation. Because of the circular symmetry of all rotating machinery, ideal solutions for the acoustic field introduce Bessel functions as shown first by Gutin. For rotor-stator combinations in a free field with equally spaced blades and vanes the Bessel function order, m, is determined precisely by the following integer relations,

$$m = nB + kV \quad \textit{axial propagation}$$

$$m = nB + kV + 1 \quad \textit{radial propagation}$$

When the Bessel function order is zero, for propagation in the directions indicated, strong radiation can occur due to geometric alignment of the blade and vane harmonic patterns. The radiated sound is always at blade passing frequency and its harmonics, while Bessel functions control the spatial pattern.

For acoustic radiation in a duct, the well-known results of Tyler and Sofrin apply with axial propagation occurring only when the blade harmonic, Bessel function order and relative mach number satisfy:

$$\frac{nB}{m} M_{rel} > 1 \quad \textit{Duct (axial) propagation}$$

Even for low speed flows, if rotor stator combinations allow m = o, those harmonics will radiate in the plane wave mode. If this Mach number criterion can be met for m ≠ o, the propagating wave is in the form of a "spinning mode".

These ideal propagation analyses predict, for a low Mach number multi-bladed rotor in a uniform flow, that tonal radiation should be very small. But, for rotor/stator or stator/rotor interactions the tonal acoustics can be quite strong. Nevertheless, such tones can be suppressed by using the well-known design rule;

$$V > 2B$$

which has the effect of preventing low order Bessel functions with potentially large amplitudes from occurring in the solution.

These precise mathematical functions provide clear rules for controlling the tonal acoustics of turbomachines. However, there remain sources of sound that are broadband, and yet to be characterized, but which may be understood better using vortex/dipole concepts.

Extension of the unsteady vortex/dipole principles to turbomachines handling real fluids with turbulence and secondary flows provides some additional useful insights into the work and acoustics. For example, while the time-average work function due to blade

motion is relatively insensitive to inflow turbulence, the acoustic behavior is quite sensitive since it is precisely the time derivative of the unsteadiness that provides the acoustic source. In addition blades in real machines generate a number of secondary vortex systems that are generally unstable and these result in unwanted mechanical losses, as well as acoustic signals associated with the time derivatives of their growth and decay. Unsteadiness in the secondary flow that occurs away from the influence of blade surfaces will produce quadrupole acoustic sources as characterized by the Lighthill stress tensor.

The applications of unsteady potential flow theory presented herein are believed to represent a unified and consistent description of the near and far–field effects for low speed turbomachines. Each topic was selected to illustrate to a particular fundamental point and to show how that understanding contributed to the larger view. As stated initially, these results are focused on cases where the stationary and moving surfaces are rigid, and where the acoustic source is compact. It is thought that this introduction will provide a sound basis for future machine development.

REFERENCES

Atassi, H.M., "The Sears Problem for a Lifting Airfoil Revisited – New Results," J. of Fluid Mechanics, Vol. 141, pp. 109–122 (1984).

Blake, W.K., "Aero-HydroAcoustics for Ships, Vols. I and II," DTRC Report 84/010, (June 1984).

Cumpsty, N.A., "A Critical Review of Turbomachinery Noise," Trans. ASME J. of Fluids Engineering, pp. 278–293 (June 1977).

Dean, R.C. and Y. Senoo, "Rotating Wakes in Vaneless Diffusers," Trans ASME J. of Basic Eng., pp. 563–574 (Sept 1960).

Duncan, P.E. and B. Dawson, "Reduction of Interaction Tones from Axial Flow Fans by Suitable Design of Rotor Configuration," J. of Sound and Vibration, Vol. 33, No. 2, pp. 143–154 (1974).

Everstine, G.C., "Structural Analogies for Scalar Field Problems," Intl. J. Num. Math in Engrg, Vol. 17, No. 3, pp. 471–476 (1981).

Goldstein, M., *Aeroacoustics*, McGraw-Hill, New York, New York (1976).

Gutin, L., " On the Sound Field of a Rotating Propeller," NACA Tech Memo 1195, Transl, (Oct 1948).

Howe, M.S., "On Unsteady Surface Forces and Sound Produced by the Normal Chopping of a Rectilinear Vortex," J. of Fluid Mechanics, Vol. 206, pp. 131–153 (1989).

Lamb, H., *Hydrodynamics*, Dover Publications, New York, New York (1932).

Lakshminarayana, B. and D.E. Thompson, "Computation of Random Unsteady Flow Field and Resulting Broadband Noise in Marine Propulsor, Cooling Centrifugal Pump, and Ventilating Fans," ONR Contract Report N00014–90–J1182 (Oct 1990).

Lighthill, J., *An Informal Introduction to Theoretical Fluid Mechanics*, Clarendon Press (1986).

Lighthill, J., *Waves in Fluids*, Cambridge University Press, Cambridge, England (1978).

Preston, J.H., "The Unsteady Rotational Flow of an Inviscid Incompressible Fluid with Special References to Changes in Total Pressure Through Flow Machines," Aeronautical Quarterly XII (Nov 1961).

Quandt, E., "The Unsteady Potential Flow Vorticity Field of Ideal Turbomachinery and its Relationship to Enthalpy Change and Blade Acoustics," DTRC Report PAS–88/66 (Dec 1988).

Rai, M. M., "Navier Stokes Simulations of Rotor-Stator Interactions using Patched and Overlaid Grids," AIAA J. of Propulsion and Power, Vol. 3, No. 5 (Sept-Oct 1987).

Tyler, J.M. and T.G. Sofrin, "Axial Flow Compressor Noise Studies," J. of Society of Automotive Engineers, Vol. 70, pp. 309–332 (1962).

Wu. T.Y. and G.T. Yates, "Literature Survey of Flow Noise Generation and Propagation in Turbomachinery," DTRC Contract Report N61533–87–2981 (Sept 1988).

INITIAL DISTRIBUTION

Copies

4 CONR
- 2 Code 1132
- 2 Code 1221

1 ONT Code 22, Remmers

2 NAVSEA
- 1 SEA 55N
- 1 SEA 56X

12 DTIC

1 Prof. H. Atassi
Dept of Mech Engrg
University of Notre Dame
Notre Dame, IN 46556

1 Prof. D.G. Crighton
Dept of Applied Mathematics and
Theoretical Physics
Cambridge University
Cambridge, England

1 Prof. Alan Epstein
Gas Turbine Laboratory
Mass Inst of Technology
Cambridge, MA 02139

1 Prof. C.M. Ho
Dept of Mech Engrg
University of California at Los Angeles
Los Angeles, CA 90024

1 Dr. M. Howe
BBN Systems and Technologies
Cambridge, MA 02238

1 Dr. David Japikse
Concepts ETI, Inc.
P.O. Box 643
Norwich, VT 05055

1 Dr. Gary Jones
PRC, Inc., Suite 700
Ballston Station
4301 North Fairfax Drive
Arlington, VA 22203

1 Prof. Joe Katz
Dept of Mech Engrg
Johns Hopkins University
Baltimore, MD 21218

1 Prof. G. Koopman
School of Engineering
Penn State University
University Park, PA 16802

1 Prof. B. Lakshrminarayana
School of Engineering
Penn State University
University Park, PA 16802

1 Prof. S. Lele
Dept of Mech Engrg
Stanford University
Stanford, CA 94305

1 Prof. D. McLaughlin
Dept of Aerospace Engineering
Penn State University
University Park, PA 16802

1 Dr. M.M. Rai
NASA Ames Research Center
Moffett Field, CA 943035

1 Prof. Donald Rockwell
Dept of Mech Engrg
Lehigh University
Bethlehem, PA 18015

1 Mr. Robert Schlinker
United Technologies Research
Center
East Hartford, CT 06108

1 Dr. Donald Thompson
Applied Research Laboratory
P.O. Box 30
State College, PA 16801

CENTER DISTRIBUTION

Copies	Code	Name
1	0112	
1	0114	
1	128	
1	15	
1	1544	
1	1502	
1	19	
1	1905	
1	27	
30	2704	
2	2723	
2	2741	
1	272T	